Turun yliopisto
University of Turku

POLYVIOLOGENS:
ELECTROCHEMICAL SYNTHESIS
AND CHARACTERIZATION

Nianxing Wang

University of Turku

Faculty of Mathematics and Natural Sciences
Department of Chemistry
Laboratory of Materials Chemistry and Chemical Analysis

Supervised by

Professor Carita Kvarnström
Department of Chemistry
University of Turku
Turku, Finland

Assistant Professor Pia Damlin
Department of Chemistry
University of Turku
Turku, Finland

Reviewed by

Professor Li Niu
State Key Laboratory of
Changchun Institute of Applied Chemistry
Changchun, P.R. China

Docent Kirsi Yliniemi D. Sc, University Teacher
Department of Materials Science and
Electroanalytical Chemistry Engineering
Aalto University
Espoo, Finland

Opponent

Associate Professor Barbara Pałys
Department of Chemistry
University of Warsaw
Warsaw, Poland

Cover picture: Nianxing Wang

The originality of this thesis has been checked in accordance with the University of Turku quality assurance system using the Turnitin OriginalityCheck service.

Now this is not the end. It is not even the beginning of the end. But it is, perhaps, the end of the beginning.

Sir Winston Churchill

Contents

List of Publications

This thesis is based on the following original publications, referred to in the text by their Roman numbers (I-IV)

I   **Wang, N**.; Damlin, P.; Esteban, B. M.; Ääritalo, T.; Kankare, J.; Kvarnström, C., **Electrochemical synthesis and characterization of copolyviologen films**. *Electrochimica Acta* 2013**,** *90*, 171-178;

II   **Wang, N**.; Kähkönen, A.; Damlin, P.; Ääritalo, T.; Kankare, J.; Kvarnström, C., **Electrochemical synthesis and characterization of branched viologen derivatives**. *Electrochimica Acta* 2015**,** *154*, 361-369.

III   **Wang, N**.; Kähkönen, A.; Ääritalo, T.; Damlin, P.; Kankare, J.; Kvarnström, C., **Polyviologen synthesis by self-assembly assisted grafting.** *RSC Adv.* 2015**,** *5* (122), 101232-101240.

IV   **Wang, N**.; Lukacs, Z.; Gadgil, B.; Ääritalo, T.; Damlin, P.; Janáky, C.; Kvarnström, C., **Electrochemical deposition of polyviologen-reduced graphene oxide nanocomposite thin films**. *Submitted to Electrochimica Acta.*

The original publications have been reproduced with the permission of copyright holders

Contribution of the author

Paper I-IV: The author did all the experiment with co-workers except the synthesis of the monomers and graphene oxide and wrote the first manuscripts and finalized them together with co-authors.

Abbreviations

WE: Working Electrode

RE: Reference Electrode

CE: Counter Electrode

ECDs: Electrochromic Devices

SAM: Self-Assembly Monolayer

IL: Ionic Liquid

GO: Graphene Oxide

rGO: Reduced Graphene Oxide

CPs: Conducting Polymers

CV: Cyclic Voltammetry

CA: Chronoamperometry

EIS: Electrochemical Impendence Spectroscopy

UV-vis: Ultraviolet–visible Spectroscopy

FTIR: Fourier Transform Infrared Spectroscopy

PM-IRRAS: Polarization modulation infrared reflection adsorption spectroscopy

AFM: Atomic Force Microscopy

SEM: Scanning Electron Microscopy

CP monomers: Cyanopyridine based monomers

BMIMBF$_4$:   1-Butyl-3-methylimidazolium tetrafluoroborate

DET: Direct Electron Transfer

MET: Mediated Electron Transfer

SNH$_2$:   cysteamine

SCNCP: 4-cyano-1-(4-isothiocyanatobenzyl)pyridin-1-ium bromide

LCP: 4,4-bis(4-cyanopyridinium-1yl) biphenyl bis-tosylate

TCP: 1,3,5-Tris(4-cyanopyridinium-1-ylmethyl)-2,4,6-trimethylbenzene tribromide

T1:   1,3,5-Tris(4-cyanopyridinium-1-ylmethyl)-benzene tribromide

T2:   1,3,5-Tris[(4-cyanopyridinium-1-ylmethyl)- phenyl] benzene tribromide

FCP: 1,1',1",1'''-(benzene-1,2,4,5-tetrayltetrakis(methylene)) tetrakis (4-cyanopyridin-1-ium) bromide

Preface

This thesis is based on experiments carried out in the Laboratory of Materials Chemistry and Chemical Analysis in the Department of Chemistry, University of Turku. The financial support from the Chemical Sensors and Microanalytical Systems graduate school (CHEMSEM), Academy of Finland are gratefully acknowledged.

Firstly, I would like to express my highest gratitude to Professor Carita Kvarnström, without her this work won't be here. Thank you for all the support, encourage and advices, you have never refused my request and always helped me to solve the problems. I would also like to thank Assistant Professor Pia Damlin, thank you for all the help in recent years, the work can't be published smoothly without the analysis and discussions. I wish to thank Professor Li Niu and Docent Kirsi Yliniemi for their careful review and valuable comments. I want to thank Professor Barbara Palys for accepting the assignment of being my opponent.

I want to express my gratitude to all my friends and colleagues in laboratory and department, who always came to my aid. Thank you very much Antti, you have taught me how to operate almost all of the equipment in the laboratory. Thank you Professors Haapakka, Lukkari and Kankareyou're your support and valuable suggestions in the previous years. I would like to thank all my co-authors, Anniina Kähkönen and Zsófia Lukacs for their excellent experimental work, especially thank you Timo Ääritalo for the continuous synthesis work. I am also grateful to Iko, Jussi, Bhushan, Sergio, Milla, Mikko and all the guys working in our group, it is very nice to work in such a pleasant environment. Thank you Kari, Mauri, Kirsi and Kaisa for all the technical help in the department.

I would like to express special and great gratitude to Professor Menghua Qin and the supervisors in my previous department for giving me the opportunity to study in Finland. Many thanks to all of my friends for your precious friendships and encourage all the times. I will never forget the happy time we have spent together.

Finally, I would like to thank my Pingping Su. You are so lovely and without you my life would be colorless, thank you for helping me to get out of the difficult times in recently years. I want to express my parents, my sister, my brother-in-law and my nephew, special thanks you for the support in my life. I want also to cherish my grandfather.

Turku, September 2016

Nianxing Wang

Abstract

Microelectronics and flexible electronics are applications that have attracted more and more attention in the today's world. The research of these kinds of electronics requires the development and improvement of existing functional materials. The viologen is one of the most frequently utilized functional materials in many different applications. Due to its unique redox property and variety of colors, the viologen materials have got worldwide attention in different fields of research.

In this work, several crosslinked polyviologen and copolyviologen film were synthesized electrochemically from different cyanopyridine based precursors. Additionally, the polyviologen based composite film was also synthesized with the introduction of graphene oxide. All of these polyviologen materials were characterized with several electrochemical, physicochemical and imaging techniques, such as cyclic voltammetry, electrochemical impendence spectroscopy, *in-situ* UV-vis spectroscopy, FTIR and Raman spectroscopy, Atomic Force Microscopy, Scanning Electron Microscopy and the contact angle technique, just to mention the most used techniques. All of the synthesized polyviologen materials showed good redox properties and unique structures, so they possess great possibility to be applied in several different fields of applications.

Due to their stable redox properties and unique porous structures, the polyviologen films have shown huge potential in the applications, both as functional materials and immobilization material, properties advantageous in varies electronics where minimization and flexibility are important parameters to achieve. By introduction of graphene oxide, the electrochemical properties of polyviologen-reduced graphene oxide based composite films could be improved making the composite structures an interesting material candidate when thinking about energy storage devices. All of these results indicate that polyviologen materials can work as multifunctional material in future applications.

Tiivistelmä

Nykyisin mikroelektroniikka ja taipuisa elektroniikka ovat saaneet yhä enemmän huomiota osakseen. Tällaisen elektroniikan tutkimus vaatii uudenlaisten ja parempien funktionaalisten materiaalien kehittämistä. Viologeeni on yksi yleisimmin käytetty funktionaalinen materiaali monissa eri sovelluksissa. Erilaisten viologeenimateriaalien yksilölliset hapetus-pelkistysominaisuudet ja kyky tuottaa erilaisia värejä ovat saaneet huomiota maailmanlaajuisesti monen eri alan tutkimuksessa. Polyviologeeni-materiaaleja on tutkittu pyrittäessä hyödyntämään viologeenijohdannaisia erilaisissa elektroniikan sovelluksissa.

Tässä työssä syntetisoitiin sähkökemiallisesti useita ristisilloitettuja polyviologeeni ja kopolyviologeenikalvoja erilaisista syanopyridiini-pohjaisista esiasteista. Lisäksi polyviologeenipohjaisia komposiittikalvoja syntetisoitiin yhdessä grafeenioksidin kanssa. Kaikki nämä polyviologeenimateriaalit karakterisoitiin useilla sähkö-kemiallisilla, fysikaaliskemiallisilla ja kuvantamistekniikoilla, kuten syklisellä voltam-metrialla, sähkökemiallisella impedanssispektroskopialla, in-situ UV-vis-spektro-skopialla, FTIR-spektroskopialla, Raman-spektroskopialla, atomivoimamikroskopialla, pyyhkäisyelektronimikroskopialla sekä kontaktikulmamittauksin ja niin edelleen. Kaikilla syntetisoiduilla polyviologeenimateriaaleilla on hyvät hapetus-pelkistys-ominaisuudet ja yksilölliset rakenteet, mikä mahdollistaa niiden käytön usealla eri sovellusalueella.

Johtuen polyviologeenien stabiileista hapetus-pelkistysominaisuuksista ja luonteen-omaisesta huokoisesta rakenteesta, niistä valmistetuilla kalvoilla on paljon sovellus-mahdollisuuksia funktionaalisina materiaaleina sellaisenaan tai immobilisaatio-materiaaleina muille kalvon komponenteille. Tällaisia kalvoja voidaan käyttää laajasti elektroniikassa rakenteiden minimoimiseen ja taipuisien rakenteiden valmistukseen. Käyttämällä polyviologeenin komposiittikalvoissa pelkistettyä grafeenioksidia, pystytään kalvon sähkökemiallisia ominaisuuksia parantamaan, mikä on erinomainen ominaisuus sovellettaessa komposiitteja energian varastoinnissa käytettäviin laitteisiin. Kaikki tulokset osoittavat, että polyviologeenit voivat toimia monipuolisina funktionaalisina materiaaleina tulevaisuudessa.

1.   Introduction

The research on viologen materials started a decade ago in the Laboratory of Materials Chemistry and Chemical Analysis. The electrochemical synthesis of polyviologens from branched cyanopyridine monomers started in 2008 and has since then been a continuous topic in the laboratory, which I picked up after joining the group in 2010. In this work, a series of crosslinked polyviologens and some viologen-based composite materials were synthesized electrochemically from different cyanopyridine based precursors. The viologen materials were characterized by several electrochemical, physicochemical and imaging techniques, which have revealed several interesting properties of the polyviologens and composites thereof that might be useful in several different fields of applications.

The background of viologen, including their synthesis, properties and application is described in Part 2. The techniques which were used in the research are described in Part 3 and the result and discussion of the research results is described in Part 4 and 5.

What are viologens? The general name of viologens is 1,1´-disubstituted-4,4´ - bipyridinium salt, which is one of the most widely used active organic material in different electronics especially in electrochromic devices (ECDs) and sensors.[1] Their unique redox properties, excellent stability, variety of colors and special structures, have inspired their application in many different fields of research.[2, 3] Switching between the differently colored redox states of viologens makes them suitable as electrochromic materials in ECDs.[4] The redox processes enable the viologens to work as mediators in sensors or biosensors.[5] Furthermore, the reductive potential enables them to work as catalyst for reduction reaction of different materials such as carbon nanotubes and graphene.[6-8] Particularly, the structure of 4,4´ -bipyridinium has been utilized as building block in the design of supramolecules due to its capability to switch between an unparalleled and an paralleled structure upon reduction.[9, 10] When the viologen is in its dication form, the two pyridine rings are in unparalleled position, with a certain angle.[11, 12] However, when it is reduced to its radical cation form, the pyridine rings will switch to planar conformation.[11] Similarly like the sigma bond (σ) or the pi-bond (π) in metalorganic complexes having ability for free rotation, the structural change between the viologen dication form and the radical cation form enables a movement of the viologen. Furthermore, if the viologens were utilized as building blocks or rings in macro molecular structures, the block/ring part can be moved along its axis by controlling the redox process. Control of movement by electrochemical redox switching is fast and efficient in comparison to chemical conversion mainly because the remaining reactant influences both the movement and

the stability of the molecule. The movement of the viologens is adjusted by an electron transfer reaction without involving reactants if made electrochemically. Owing to the good stability of viologens and easy redox tenability these molecules are frequently applied in the design of artificial molecular machines.[13, 14] Viologen based molecular machines are commonly studied in selective catalysis and as molecular shutters, making viologens an essential building block in supramolecular chemistry. Recently viologens have achieved an increased attention mainly due to the numerous possible ways of building polyviologen derivatives.

Today the development of electronics is focused on portable, flexible and multifunctional devices; this is why organic based electronics is studied extensively. In the research on viologen materials, an increasing attention has been paid to polyviologens, since such structures not only possess the special properties of viologens, but moreover shows extended properties as improved flexibility and stability, high light transmittance together with easy preparation and derivatization through electrochemical synthesis, all important properties when utilized in electronics.[15, 16] The electrochemically synthesized polyviologens have all the advantages above, and additionally, can be deposited as films directly on the substrate intended for application even in complicated patterns.

The work presented in the thesis is divided into two parts: Firstly the electrochemical synthesis of various viologen materials; including the crosslinked polyviologens (TPV, PolyT1 and PolyT2), copolyviologen films (CoPV), and polyviologen-based composite materials (PV-rGO). Secondly different cyanopyridine based monomers were utilized in the electrochemical synthesis, using both aqueous solution and ionic liquid as electrolyte in electropolymerization by different methods. The obtained polyviologen film materials were characterized by different electrochemical and physicochemical techniques.

This work comprises mainly three different approaches to produce viologen materials electrochemically. Namely the synthesis of polyviologen films of network structures based on branched cyanopyridine monomers, the synthesis of ordered polyviologen structures on top of self-assembly monolayer (SAM) modified electrodes and the synthesis of composite materials of polyviologen/reduced graphene oxide using room temperature ionic liquid (ILs) as electrolyte. In the first mentioned case, the formed crosslinked polyviologen films have a unique porous structure. By changing the initial monomer or introducing a second monomer, the network cavities can be tuned according to the size of the molecules or materials intended to be immobilized in the network structure (article I). For the second method, a well-ordered polyviologen film was formed on top of a self-assembly monolayer modified electrode, which provides

the potential of the material to be applied in ultrathin organic electronics (article II). In the last method, a composite material was synthesized by polymerizing cyanopyridine derivatives in presence of graphene oxide (article IV). The composite materials showed enhanced conductivity and stability which broadens the application field of polyviologen materials: i.e. the composite material shows promising properties to be utilized as energy storage materials.

The redox property is the most essential characteristic for viologen materials. In this work, all of the synthesized polyviologen materials have been investigated by electrochemical techniques. Based on the results, it could be proved that the crosslinked polyviologen films undergo a characteristic two step well defined reversible redox processes showing good stabilities. For the polyviologen film, synthesized on top of a SAM modified electrode, only the first redox process was detectable. Furthermore, when the other materials were introduced into the polyviologens to form the composite materials, the redox property of the viologen was affected. As an example, when the reduced graphene oxide (rGO) was employed, the redox property of the resulted composite material was enhanced comparing to that of pure polyviologen films.

Furthermore, special efforts have been put on modifying the structures of the polyviologens, thus obtaining derivatives with tuned intrinsic properties needed for different applications. Influence of extrinsic factors on material properties were also studied; as an example by adjusting the anions in the electrolyte, the polyviologen redox potentials can be shifted and the material can maintain its radical cation form for longer times. This finding in combination with the unique porous structure of the polyviologen films makes them interesting materials also in sensor applications or in fuel cells in the future.
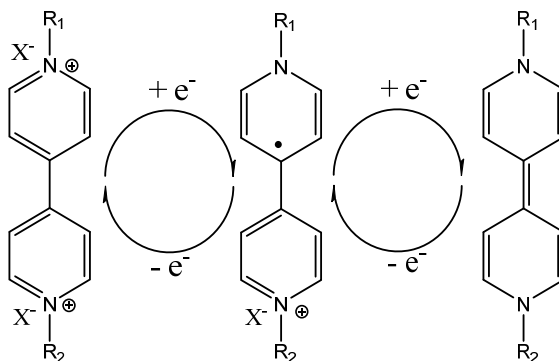
One aim of this research is to apply the polyviologen films as electronically active host materials for molecule immobilization in electronic and optoelectronic devices. The immobilized molecules and electron mediator material can be combined together in the polyviologen films, which will simplify the fabrication process of the devices. In order to characterize the structures of the polyviologen films, especially the cavities, electrochemical measurement and microscopic techniques were utilized. Based on the electrochemical study using different counter anions upon charging-discharging and on the SEM analysis (**Paper III**), it was proved that by changing the design of the initial monomers or precursors, the resulting polyviologen films can contain different sized cavities enabling the material to be used as both mediator and immobilization/matrix material.

Besides the published work presented in this thesis, other properties of the synthesized polyviologen materials, such as the stability, pH effect and hydrophobicity have been studied. All of the results show that the polyviologen materials especially the crosslinked polyviologen films can maintain excellent redox properties, and by introducing functionalities/functional groups, the polyviologen materials adapt new properties. By this work, it was proven that polyviologen materials can work as new, interesting functional material in future research, especially in the field of organic electronics.

2. Background

2.1 Viologens

Viologens, usually named 1,1´-disubstituted-4,4´ -bipyridinium salts, have been in focus of increasing attention due to their unique properties.[1-3] The distinct color change and stable redox property are the two main features of viologens and reasons to why it has been frequently used functional material. In the last three decades, the viologens have been widely utilized in electrochromic devices,[17-22] sensors,[5, 23-26] fuel cells[27-30] and other electronic devices,[6, 31-33] additionally, due to their unique structure they are also utilized in supramolecule structures.[34-36] The characteristic redox process, showing three different forms of viologen is shown in Scheme 1.

Scheme 1. Three redox forms of viologens (From left to right: dication form, radical cation form and neutral form)

The most important property and the key feature of viologen is their redox response. As shown above in Scheme 1, viologen undergoes two successive reduction processes, which contain two single electron transfer steps. The first step, is fully reversible during cycling, a property that is frequently utilized when viologen is applied in varies electronics. The second step is quasi-reversible, which can be elucidated by the change in the steric structure of viologen resulting in a less soluble compound during the second redox process.[1, 2] However, it should be mentioned in this work, the second redox process has shown good reversibility; which will be described further in Part 4. The three different redox forms of viologens are: the dication form, the radical cation form and the neutral form.[1] The dication form is the most stable form, however the radical cation form is the most interesting state, which possesses the key properties utilized in different areas of applications i.e. redox property, solubility, electrochromism, morphology. The research on neutral viologens is quite rear,

however, it still need to be mentioned that neutral viologens can work as a reductive agent, which can be utilized to reduce or dope other materials.[6, 37]

The term viologen was firstly used by Michaelis in 1933 influenced by the unique color change taking place during the redox reaction.[2] Since then viologens have been studied intensively in electrochromic devices and as redox indicators. The main factor which determines the colors of viologens and viologen derivatives is their functionalization. The radical cation form is blue if functionalization is made by non-conjugated alkyl or benzyl groups.[38-40] The same redox state can also appear green if the substituted group is p-cyanophenyl[21, 41, 42] and violet if the substituted groups are phenyl or COPh.[39] Another factor which affects the absorption spectra is the dimerization of the radical cations, leading to a broader absorbance in the visible region of the spectrum.[2] The dication form of viologen can also be colorful, based on the electron transfer between the viologen unit and the corresponding counter ions[43] i.e. light red color in presence of I$^-$ or NH$_2$Phenyl counter ions.[44] There are quite few studies on the colors of viologens in their neutral form one of them mentioned an aryl functionalized viologen that turns viologen red due to the resulting extended conjugated structure.[45] Crystalline viologen structures show their own spectral characteristics that will not be discussed here.[46]

The observed color changes are a result of a change in the electron distribution on the pyridine rings due to substitution, a change completely dependent on the type of functional group attached. Important properties as the redox potentials and the solubility of the viologens will be modified, i.e. the length of an attached alkyl chain reduces the redox potential of viologen simultaneously as the solubility increases.[45]

Beyond the viologens, there are a series of electrochromic materials which have also been studied and applied in the different applications, such as metal oxides, hybrid materials, and metallopolymers.[47-51] Each material has its own advantages and limitations, for example, the metal oxides such as Prussian Blue and WO$_3$ have been widely utilized in smart windows and electrochromic displays, due to their good stability.[52, 53] However, the difficulty of the redox adjustment and the higher cost of the materials limited their applications. In comparison to the inorganic electrochromic materials, viologens are more favorable in manufacturing, due to their light weight, lower cost and adjustable redox potentials.[3, 54]

The number of viologen materials synthesized and characterized in recent years is large, and their field of application has expanded. Synthesis of rotaxane in supramolecules is accomplished utilizing the steric change taking place during the redox processes of viologen. Furthermore, it has been shown the
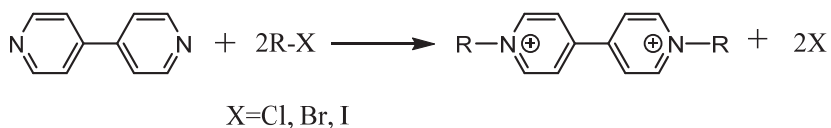
hydrophobic/hydrophilic properties of viologens are changing during the redox process, an interesting fact for wettability research.[55] Moreover, the resistance to biofouling enabled the viologens to be utilized in corrosion protection, and viologens can also be used as catalyst material. All of these works has shown that the viologen has huge potential as a functional material in various applications in the future.

2.2   Synthesis of viologens

2.2.1 Organic synthesis

Traditionally viologens have been synthesized using chemical methods, such as Menschutkin reaction,[56-58] Zincke reaction[16, 42, 59] and Winters reaction.[60, 61] Through these methods, many different viologen materials were designed and synthesized.
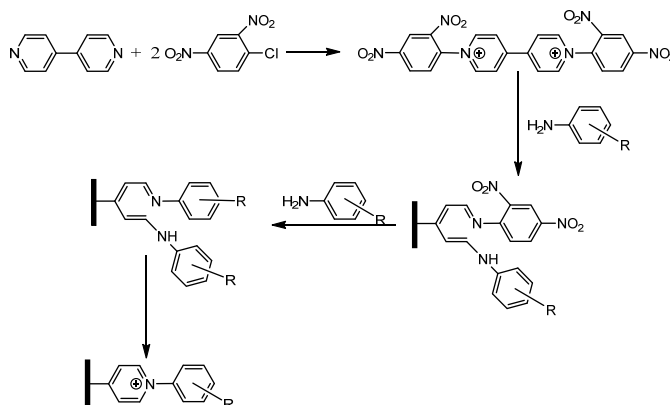
The mechanism of Menshutkin reaction is shown in Scheme 2 below. Viologens can be prepared by the reaction between 4,4′-bipyridine and an alkyl halide, a counter anion which is utilized to balance the charge of the resulting viologen, an anion that can be changed by ion exchange. By this reaction viologens can be easily prepared even as organized thin layers on top of different modified surfaces, especially on self-assembly layers. A series of viologen monomers are prepared using this method, e.g. the Takuya Masuda´s group studied the performances of viologen synthesized on a self-assembly monomer modified surface. The synthesized viologens showed good catalytic properties.[62-65] Similar work can be found by E. T. Kang's group, where viologens were formed on top of polypyrrole, by which the conductivity of viologens were enhanced.[66, 67] However, by this reaction the structure of the viologen derivatization was limited to alkyl, limiting the tuning of redox potential and color. In order to synthesize different kinds of viologens, the Zincke reaction was introduced.[7, 42, 59, 68]

X=Cl, Br, I

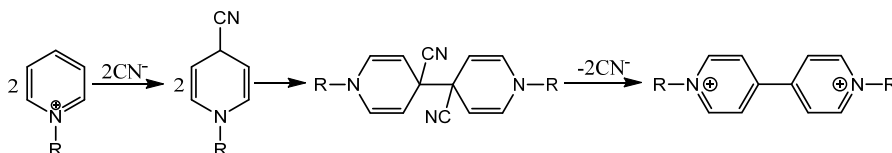**Scheme 2.** Synthesis of viologen from 4,4′-bipyridine and alkyl halides [7, 42]

Comparing the Menshutkin method, to the Zincke method is complex. However, by the latter reaction, phenyl and alkyl substituted viologens can be synthesized. In Scheme 3, the procedure for synthesis of a phenyl substituted viologen is shown: firstly 2,4-dinitrochlorobenzene reacts with 4,4-biypridine after which the viologen (mono-substituted or di-substituted) is formed. The resulting viologen will then react

with aniline, to form pyridine. After that, by continuously adding aniline, the 2,4-dinitrobenzene will be formed as 2,4-nitroaniline. Continuing the reaction, phenyl substituted viologen will be formed. It should be mentioned that when mono-substituted viologen is synthesized, for example the 1-aryl-1′-alkyl viologen, it is preferable to add the aryl substitute group before attaching the for alkyl groups.[1] A series of viologen materials were synthesized by this method, especially dendrimers and cucurbiturils.[11, 69] Lorenz Welder's group has synthesized numerous dendrimers,[7, 42, 70, 71] and the NMR spectra and electrochemical characterization proved that the viologen can be synthesized with alternating structure.

Scheme 3. Synthesis of viologen from phenyl substituted groups by Zincke reaction[11, 16]

Another method of viologen synthesis is the Winters reaction, shown in Scheme 4. The 1-substituted pyridine is firstly reacted with the cyano anions and by removing one hydrogen ion; the 1-substituted-4-cyanopyrdine is formed. After that, two 1-substituted-4-cyanopyrdines can couple together and after removing the two cyano groups, the 1,1- disubstituted viologen will be formed. This method was widely utilized to synthesize polyviologens, and this is also the major route to produce Paraquat (methyl viologen dichloride).

Scheme 4. The synthesis of viologen with coupling of 1-substituted pyridine cations.[61]

Additionally, beyond the viologen monomers or polymers, viologen materials can also be modified into polymers or large molecules as the pendant group by the synthesis reactions described above.[72-76] One of the important examples is the conducting

polymer: the electrochemical polymerization of thiophene substituted by a viologen pendent and the electrochemical and electrochromic properties of such structures have been reported.[77-80] Serge Coniser, et al. designed a series of polypyrrole based polymers having viologen as pendant group for sensor applications[81-86]. Combining conducting polymers and viologen, enhanced the electron transfer between the pendant viologens and the polythiophene backbone leading to an increased detection limit. Furthermore, E.T. Kang also studied the application of viologen or polyviologens as pendant group on the conducting polymers (polypyrrole) and their sensor applications,[66, 67, 87-90] which also showed good electron transfer properties.

2.2.2 Electrochemical synthesis

In 1977, conducting polymers (CPs) were firstly discovered, and due to their excellent conductivities,[91] these materials got worldwide attention immediately. For the discovery and development of CPs, Alan J. Heeger, Hideki Shirakawa and Alan G. MacDiarmid were awarded the Noble Prize of Chemistry in 2000. In the last two decades, many new CPs and derivatives thereof were synthesized, and have been utilized in varies electronics and applications.[21, 47, 92-96] In the research of conducting polymers, electrochemical synthesis has received increasing attention in recent years. Both chemical synthesis and electrochemical synthesis have shown their own advantages and disadvantages. By the chemical routes, the products can be obtained with a precise structure, as in the synthesis of a supramolecule having metaproperties;[97, 98] furthermore, the products can be synthesized in large scale, which is an important factor for commercial applications. On the other hand, the unique qualities of electrochemical synthesis including low cost, high energy efficiency,[99, 100] enables an affordable way for one step synthesis of films directly onto the substrate to be used in different applications. Moreover, the working condition of electrochemical synthesis is usually mild and there are fewer impurities remaining after the polymerization process,[100, 101] which is favorable when thinking about further analysis and applications. The electrochemical synthesis is performed by oxidation/reduction of the monomers, which can be accomplished by applying a certain potential on the working electrode (positive/negative). The electrochemical synthesis of conducting polymers involves mostly the oxidation of a monomer unit, only a few of them can be synthesized by cathodic electropolymerization (reduction).[99]

The electrochemical characterization techniques are playing a central part in analysis of materials. By the electrochemical techniques, such as Cyclic Voltammetry (CV), Chronoamperometry (CA), Electrochemical Impendence Spectroscopy (EIS), the electrical parameters of the materials, such as the redox potentials, conductivity,

resistances and capacitance can be measured. Especially, by combining these techniques with spectroscopic techniques, named *in situ* spectroelectrochemical measurement, the resulting polymer/film can be simultaneously analyzed during the synthesis process or immediately after synthesis directly from the electrode substrate. In this work, *in situ* UV-vis, FTIR and conductive measurements have been utilized to characterize the performance of the electrochemically synthesized polyviologens; this is described in more detail in Part 3.

In 1964, Kosower and Cotter demonstrated the synthesis of viologen by coupling of two cyanopyridines,[102] thereby demonstrating that also electrochemical synthesis of viologen from cyanopyridine based monomers (CP-monomers) can be successfully performed. The mechanism of the reaction is similar to the Winters reaction which was shown above in Scheme 4. The electrochemical coupling is made by reduction of the CP-monomers forming radicals that will couple to dimers. After removal of the –CN groups a viologen unit is formed. The process is continued by further coupling of CP-monomers growing the chain length to oligomers and polymers.[103-106] As described above, the performance of the viologen can be strongly affected by the substituted group. A series of cyanopyridine monomers have been designed and synthesized in the group and are listed in Scheme 5 below. The ones having a branched structure were designed for the electrochemical synthesis of crosslinked polyviologens or copolyviologens. The linear CP monomers shown in Scheme 5 were designed for viologens formation on modified electrode surfaces for more specific structures through self-assembly. All monomers contain one or more cyanopyridine group, through which the electrochemical coupling takes place.

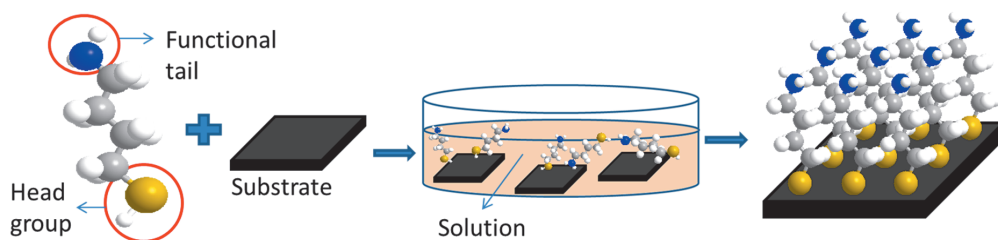| Monomer structure	Name	Abbrev. monomer/polymer
	1,3,5-Tris(4-cyanopyridinium-1-ylmethyl)-2,4,6-trimethylbenzene tribromide	TCP/TPV
	1,3,5-Tris(4-cyanopyridinium-1-ylmethyl)-benzene tribromide	T1/PolyT1
	1,3,5-Tris[(4-cyanopyridinium-1-ylmethyl)- phenyl] benzene tribromide	T2/PolyT2
	1,1',1'',1'''-(benzene-1,2,4,5-tetrayltetrakis(methylene))tetrakis(4-cyanopyridin-1-ium) bromide	FCP/PFV
	4-cyano-1-(4-isothiocyanatobenzyl)pyridin-1-ium bromide	SCNCP
	4,4-bis(4-cyanopyridinium-1yl) biphenyl bis-tosylate	LCP

Scheme 5. A series of cyanopyridine based monomers

2.2.2.1 *Self-assembly monolayer*

In this work the electrochemical synthesis and growth of polyviologen materials was also made on modified electrodes covered by a self-assembled monolayer, which is formed through the reaction between the cysteamine (SNH_2) and isothiocyanate based cyanopyridine monomers (SCNCP) (SNH_2-SCNCP). SAM, firstly reported by Nuzzo in 1983,[107] offer unique advantages as easy preparation of large or patterned

substrates.[108, 109] The substrates can be of metal, metal oxide or semiconducting materials; [110-113] there are series of monomers which can work as anchor structures to form SAM. A monomer which can undergo SAM process should at least contain two parts: a head group and functional tail. The head group should have the ability to form the stable bond with the corresponding substrate, one of the most utilized head group is the organosulfurs (thiols, disulfides and sulfides), since it can react easily and form stable bonds on the surfaces of gold or platinum. The functional tail should have special properties or structure depending on the demand or should be possible to modify in following steps.[113] The middle part linking head and tail can consist of an alkyl chain or other functional groups, which length strongly affect the property of the SAM, especially the electron transfer.[114, 115]

The SAM does not only allow an easy and simple process to modify the surface of different substrates, but also offers a method to change the morphology and the energy levels of the material surface. The SAM process is sketched in Scheme 6: the monomer is firstly dissolved in a proper solvent, after that the corresponding substrate is immersed in the solution for a certain time, which can prolong from minutes to days depending on the monomer and the substrate under study. During this immersion process, a strong covalent bond can be formed between the head group of the monomer and the substrate surface. The mechanism can be divided into two steps: in the first step the chemisorption is very fast, during which most of the monolayer is formed. This process is assumed to be controlled by diffusion and the kinetic is limited by the concentration of the monomer and the reaction between the head group and the substrate. The second step, which is a crystallization process is very slow comparing to the first step. In this step, the disordered monolayer can rearrange to well-ordered structures.[116] The ordered monolayer will be formed for further application or modification.

Scheme 6. Procedure for SAM formation on a substrate.

In electrochemistry, SAMs are widely used to modify the electrode surface for special purposes. For instances the work function of a substrate can be adjusted thus allowing a reaction i.e. electropolymerization to take place at a lower potential leading to a

better coverage of the substrate alternatively to formation of longer polymer chains. Furthermore, the characteristic thickness of a SAM is around 1-3 nm, which enables the preparation of flexible and ultra-thin electronics.[109] The electrochemical properties of viologen-based SAM films has been studied for a long time, and a series of monomers which contain one or several viologen units have been synthesized with unique design and applied in various electronics[28, 109, 113, 117-119] where this redox active material played an important role as electron relay in an electrochemical process.[120] In these monomer structures the viologen unit was present either in the middle or as tail groups, in which their performance were limited. In this work the intension was to broaden the field of application of viologen materials by the SAM method. An ordered polyviologen film was electrochemically synthesized using SAM of a specially designed and synthesized cyanopyridine linker. The synthesized viologen film does not only show good redox property but also have the ability to be applied easily on different substrates using the same linker structure; furthermore, with changing the CP-monomers, the property of the viologen films can be easily changed for different demands. This work will be further discussed in Part 4 in detail.

2.2.2.2 *Ionic Liquids*

Room temperature Ionic Liquids (ILs) are new solvent candidates which are widely employed in an increasingly wide range of chemical fields nowadays due to their unique properties, especially as electrolytes in electrochemistry. Even if the first described room temperature IL was reported already 1914, ethylammonium nitrate [$Et(NH_3)$]·[NO_3] with a melting point of 12°C, the extensive attention on ILs started only a few decades ago and since then a huge amount of new ILs were synthesized and applied in various research areas.[121-123].
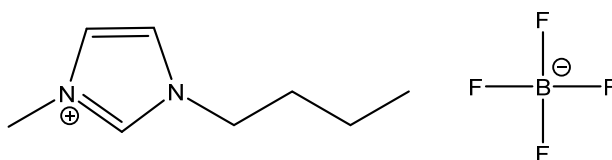
The special merits of ILs, which are usually classified and grouped as follows: i) they are composed entirely of ions (salt), a wide range of both organic and inorganic anions and cations are possible to combine together. Additionally, by altering the combination of the ions, it is even possible to tune the solvent properties to special aims. ii) their intrinsic conductivity is high. Unlike the other solvents, it is not necessary to add a separate salt to increase the conductivity of the solution. iii) they are immiscible with most organic and inorganic solvents. iv) they have high thermal stability and no vapor pressure.[44, 124] These advantages enlarge the application of ILs, and strengthen also their role in electrochemical measurements. Due to the large potential window, good stability, high polarity, the ILs are widely utilized in applications such as batteries, electrochromic devices, supercapacitors and other electronics.[125-129]

However, as a new kind of solvent, there are still some challenges to be solved. As different ions are employed, the toxicity and pollution of the ILs should be considered. In recently year, more and more 'green' ILs were synthesis from natural products.[130] Another problem is their sensitivity to moisture, when H_2O is adsorbed into the IL; the electrochemical window will significantly decrease. When ILs are utilized in the electronics, the sealing of the device is one critical procedure. Furthermore, the viscosity of ILs is usually higher than for aqueous and organic solutions, which strongly effect on the mass transfer in electrochemistry if the ILs are utilized as solvent. The extremely slow rate of mass transfer leads to very low currents, which complicates the electrochemical measurement, especially in electrochemical polymerization reactions.

A few reports on the combination of ILs with viologens can be found from recent years. The different ILs were introduced into varies electronics as electrolytes, especially in the electrochromic devices.[20, 131-133] By employing ILs, the thermal stability and transparency properties of the ECDs were highly improved. Furthermore, with the large potential window, the switch in different redox forms can be achieved in higher potential, which are usually limited in the case of aqueous solutions. Additionally, viologens can also work as the component materials in the design of ILs.[134, 135]

In this work, IL was utilized as solvent for electrochemical synthesis of polyviologen and reduced graphene oxide composite. Graphene has become one of the most attractive materials after it was firstly isolated in 2004.[136] From that day on, graphene has got worldwide attention due to its unique two dimensional structure and unique properties, such as high conductivity, good mechanical strength, large specific surface area and high transparency.[137-140] The graphene and its derivative materials, especially Graphene Oxide (GO), have been widely studied and applied in various electronic devices and other applications.[141-146] One of the most attractive research topics of graphene is its utilization in composite materials.[144, 147-149] The graphene can be prepared and isolated with different methods including micromechanical or chemical exfoliation of graphite, chemical vapor deposition (CVD) growth, and GO usually synthesized by oxidation of graphite. In comparison to other graphene derivative materials, GO has shown unique advantages such as easy preparation even in large scale.[150, 151]However, on the surface of GO, there are plenty of hydroxyl and epoxy groups attached which are easily affected by the variation of the preparation process.[152] In order to remove these oxygen containing functional groups, the rGO can be prepared by chemical, electrochemical, thermal, or photocatalytic reduction of GO.[150, 151, 153-157]

The GO can be solved solely in deionized water, however, when other ions are introduced into the solution, the GO are usually aggregated and switched to unsolvable state. In order to solve this problem, IL is introduced as the solvent in the electrochemical synthesis of polyviologen and rGO composited film. One of the biggest differences of using ILs as electrolytes is the lack of a neutral solvent. In conventional electrolytes the ions are often considered to be fully dissociated and surrounded by solvent molecules. In ILs, on the other hand, the ion transport is not necessarily as simple and it is highly likely that the cations and anions are not as fully dissociated from another as they are in conventional electrolytes. The 1-Butyl-3-methylimidazolium tetrafluoroborate (BMIMBF$_4$) was used as IL, structure shown in Scheme 7, and more details about the obtained results will be shown in Part 4.

Scheme 7. Molecular structure of 1-Butyl-3-methylimidazolium tetrafluoroborate.

2.3   Electrochemical properties of viologen

The electrochemical properties of viologens have attracted research attention for a long time and has therefore become a frequently utilized functional material.[1, 2] It has been described above in the previous parts that the redox potentials can be adjusted through substitution by functional groups[3]. However, once the viologens are trapped in a molecule or polymer their redox properties can be affected by several different parameters, such as electrolytes, anions, pH and substrate materials.[18, 133, 158, 159] An important feature of viologen is the structural change taking place during its redox process: two pyridine rings are   turned parallel from being slightly twisted upon reduction of the dication form to the radical cation form.[160, 161] This phenomenon was supposed to influence the conductivity; solubility and redox property of viologens. In order to characterize the electrochemical properties of the synthesized viologen materials in this work the effect of anions on the redox property were studied.

2.3.1 Redox property

The electrochemical properties of viologens involve two redox processes and corresponding three redox forms, which have been depicted above in Scheme 1. The first redox step, involving one electron is totally reversible and can be switched back and forth   several times without material degradation.[1, 2] However, the second

reduction step is usually quasi-reversible or irreversible, which can be explained by that viologen in its neutral form is usually insoluble.[1, 2, 162] The redox potential is the key parameter which determines the application of the viologens. The redox potentials (E_{pa}, E_{pc}) can be measured by electrochemical methods, such as cyclic voltammetry, and a typical redox process of polyviologens is shown in Figure 1 below. Based on the Nernst equation:

$$E = E^0 + \frac{RT}{nF} \ln \frac{C_O}{C_R} \tag{1}$$

A reversible redox process can be confirmed by the peak potential

$$E_p = E_{1/2} - 1.109 \frac{RT}{nF} = 28.15/n \; mV \text{ (at 25°C)} \tag{2}$$

Under some conditions, peak currents are too broad in order to determine an accurate peak potential value. This is why it is easier to detect the half-peak potential $E_{p/2}$, which is the potential at the half current of the peak current value (as an example, $E_{pc1/2}$ in Figure 1).

$$E_{p/2} = E_{1/2} + 1.09 \frac{RT}{nF} = E_{1/2} + 28.0/n \; mV \text{ (at 25°C)} \tag{3}$$

Thus, by summarizing equation 1 and 2, the peak potential can be determined.

$$E_p - E_{\frac{p}{2}} = \left(E_{1/2} - 1.109 \frac{RT}{nF} \right) \left(E_{1/2} + 1.09 \frac{RT}{nF} \right) = 2.20 \frac{RT}{nF} = \frac{56.5}{n} mV \tag{4}$$

For a reversible process, the potentials should be independent of the scan rate, and according to the Randles–Sevcik equation, the peak currents should be proportional to $v^{1/2}$.[163] The peak current i_p is:

$$i_p = (2.69 * 10^5) n^{3/2} A C D^{1/2} v^{1/2} \tag{5}$$

At 25°C, A is the area of the electrode in cm^2, C is the concentration in mol/cm^3, D is the diffusion coefficiency in cm^2/s, and v is the scan rate in V/s.
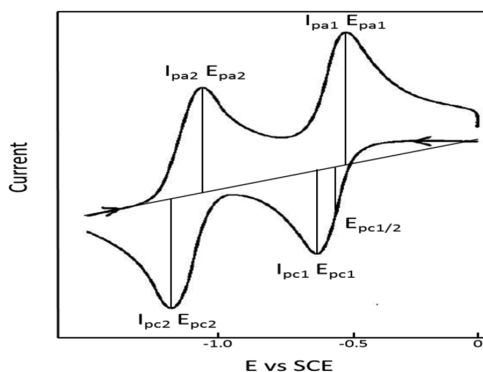
Figure 1. Cyclic voltammetric response of a N,N'-dialkyl-viologen salt[164]

The redox potentials, especially for the first redox couple, are very important in the application of viologen in varies electronics. For example, it is important that the viologen undergo the first redox reaction at relatively low potentials if the viologens are utilized in electrochromic devices, this for easier control of the device using less energy.[165] Furthermore, in biosensor or bio-fuel applications, it is important to employ viologens undergoing redox reactions at potentials close to the once of the biomaterials. As a result, the electron transfer will be more efficient between the surface and the reactant.[166, 167] The second redox couple has engaged much less research than the first one, due to the quasi-reversible process and the higher reductive potential, which have limited its application. However, the strong reductive property can be used to modify the Carbon Nanotubes.[6] In order to study the reductive property, the neutral formed extended viologen was successfully synthesized.[37] Additionally, the second redox process is frequently studied in molecule electronics in supramolecule chemistry.

The stability of the different viologen redox states is another important factor to study, as the viologens are usually utilized as derivatives of different structures. The sustaining time of both redox forms of viologen can differ quite much.[1] Especially in electrochromic devices, the stability of viologen in its radical cation form is crucial. For some derivatives the viologen can be maintained in its radical cation form for several months, like the heptyl viologen.[49] In this work, switching between the different redox states of the viologen film materials has been studied by cyclic voltammetry for several cycles in order to study the stability of the films upon continuous cycling. Polyviologen films were also characterized by the chronoamperometric technique by which it was proven that both the structure and the counter ions have a big influence on both the redox potentials and on the stability of

the different redox states. The effect of anions will be described more in detail in the next section.

As mentioned above, by changing the substituent groups, the redox potential of viologens can be changed, and numerous viologen materials have been designed and synthesized for this reason.[2, 17, 168-171] In this work, the linear CP-monomer (LCP) was designed (shown in Scheme 5) and electrochemically synthesized to linear oligomeric viologen films. A second approach in this work has been to modify the viologen properties by incorporation of new materials, as rGO, to form hybrid/composite materials. The introduction of rGO into the viologen redox material mainly influenced the charge transfer in the composite structure. GO is simultaneously reduced to rGO during the electrochemical polymerization process. Incorporation of rGO leads to improved electrochemical response and changed morphology of the composite film. The details will be described in Part 4.5 and Part 4.6 below.

Besides the three redox forms, there are some special phenomenon taking place during the redox process which also affect the performance of the viologen materials. The first one is the comproportionation causing a dimerization of to viologens in their radical cation form. Dimerization has been confirmed by many different techniques[172-174] and is supposed to occur when two viologen units are close enough to interplay. In this work such a phenomenon has been observed with short branched structures of polyviologens,[175] and will be described later in part 4.3 focusing on UV-vis studies on polyviologen materials. The dimerization of viologen units is also expected to increase the stability of the viologen in radical cation form, which might be favorable in certain applications.[9, 116]

Another phenomenon taking place during the redox process is the structural change between the two pyridine rings.[160, 161] When the viologen is in its dication form, the two pyridine rings in the viologen are linked together at a certain angle. However, when the viologen unit is reduced into its radical cation form, the two pyridine rings are twisted into a more planar configuration. This phenomenon gives the viologen the ability of movement when charged and based on this property, a series of specific molecule machines were designed.[9, 36, 176] Furthermore, it has also been proved that this structure change can modify the hydrophobic/hydrophilic property of the viologens.[161, 162, 177]

In this work, the redox parameters of all the viologen materials were measured and analyzed. All of the electrochemically synthesized viologen materials under study showed good redox property meaning well defined, reversible and reproducible redox states with switching at moderately negative potentials. All properties indicate and

point at a remarkable prospective of these materials in varies electronic application, the details will be described in Part 4 below.
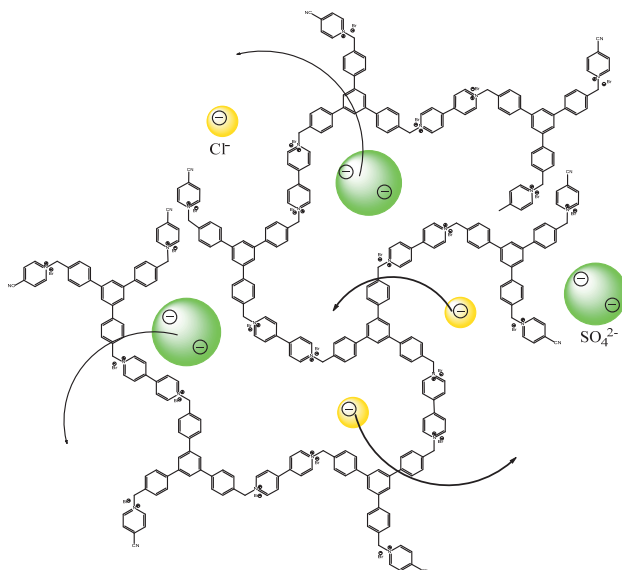
2.3.2 Effect of anions

Beside the substituent groups, anions are another important component in the viologen materials. It was already mentioned that anions influence the color of viologens in some cases. However, anions have also a significant effect on the solubility and on the electrochemical properties of viologen materials. Anions do not affect the precipitation process, but affect the aggregation of viologens.[55] As an example, chloride can induce heptyl viologen precipitation while bromide does not.[2] After realizing that the redox performance of viologens can be effectively tuned by anions, the interaction between the viologen unit and varies anions has been studied insensitively.[103]

A series of results have proven that the redox properties of viologens are influenced by anions.[2, 169, 178-182] It is assumed that when viologens are undergoing a redox process, anions will bond to the viologen unit by an ion specific binding energy. Since viologens with various different structures have been synthesized and studied under quit different conditions (film thickness, pH etc.) it is hard to draw conclusions from the published data concerning the relationship between viologens and anions.[2] However, the sizes of the anions have shown to strongly influence on the redox property of the viologens, i.e. it was shown that the reduction potentials shifted more negative when the size of the anions are increased.[103, 183-185]

$$SO_4^{2-}<Cl^-<ClO_4^-<PF_6^-.$$

On the other hand, in the last two decades, use of viologens in sensor applications have attracted quite much attention, where anions were studied as the detective reactant in viologens.[103, 106] Tomokazu Iyoda´s group has studied the influence of halide ions on polyviologens based on crosslinked polyviologen films.[103] It has been proven that the cavities in the films can be controlled by the initial structures of the monomers or precursors. Inspired by their work, the effect of varies anions on the different polyviologens were also studied in this work, mainly with focus on diffusion properties of different anions in the polyviologens. As viologens are widely utilized functional materials they are commonly applied as one part together with other materials. Traditionally viologens were immobilized in polymers or membranes, which not only enabled the process of viologen and increased the way of material

construction but also limited the performance of viologens. In this work the application of viologens was taken one step further by applying polyviologens as host films for other functional materials. Therefore, the cavities of the polyviologen films are an important parameter in the viologen precursor design. Two branched polyviologen derivatives were both electrochemically synthesized and characterized in different electrolytes and the diffusion of the anions was studied. As shown in Scheme 8, anions can move in and out from the inner cavities which were formed by the branched network like polyviologens. When reducing the polyviologen film anions were expelled out from the film, after removal of the applied potential ions can freely move back into the film. A small ion has higher mobility comparing to the large ones if solvatisation is not taken into account, and moves more easily in the large cavities. From the analysis of the performances of the polyviologens in presence of different sized anions, it was proven that the cavities in polyviologens can be controlled by differently branched precursors or monomers. These kinds of branched polymer structures have shown huge potential as host materials. More details of this part of the work are described in Part 4.

Scheme 8. Movement of anions in polyviologen

2.3.3 Conductivity

In the design and manufacture of electronics, the conductivity of the material is an important parameter. In viologens the two pyridine rings are nonplanar and this is why the π orbital cannot be formed easily, and the conductivities of the viologens are usually quite weak. In order to solve the problem, a series of viologens were designed

and several new materials, such like conducting polymers, CNT and graphene, were introduced as host or counter parts.[15, 67, 186-188] It was already described above that viologens can be applied as pendants on a conducting polymer in order to increase the electron transfer ratio. Furthermore, also viologens having conjugated moieties for extension of the π-conjugated structures have been designed.[189] In this work, the rGO was introduced into polyviologen, in order to increase the conductivity of pristine polyviologens films. The composite film was successfully polymerized and characterized, and the results are shown in **Paper IV**.

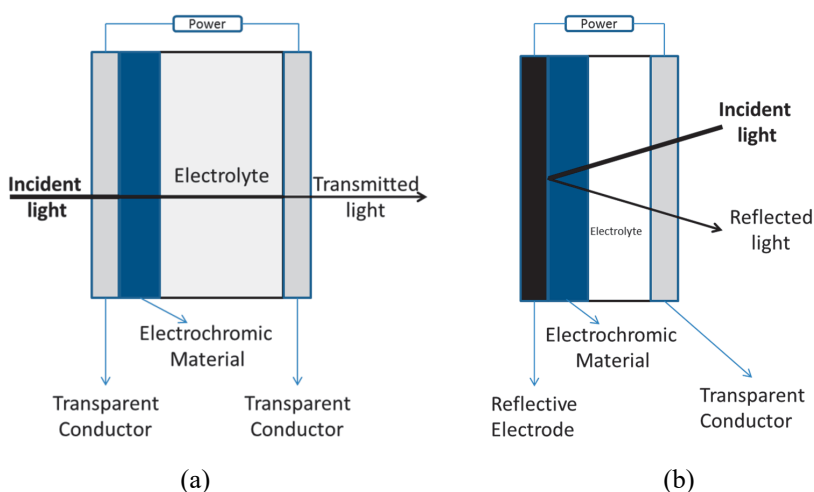## 2.4 Applications of viologen

2.4.1 Electrochromic devices

Electrochromic devices (ECDs) are a common term for electronics that can fade out or switch the color by passing a current or applying a potential to the active electrodes.[21, 165] Generally there are two categories of ECDs, based either on transmittance or on reflectance, as shown below in Scheme 9. A large variety of ECDs have been designed and quite many of them have also been commercialized. For example, electrochromic smart windows have been installed in cars, trains and airplanes (Boeing 787),[21, 190, 191] that are based on the first type of device. The second device type, is usually designed for smart mirrors, such as anti-glare mirror.[118] Plenty of parameters effect and limit the performance of ECDs, such as contrast ratio, coloration efficiency, response time, cycle life and energy consumption,[18] but in this work, the research is focus on the materials.

The electrochromic materials which have been utilized in ECDs can roughly be divided into three different types: materials which are soluble in reduced and oxidized state (Type I), materials which are only soluble in one redox state (Type II) and materials which are solid in both of its redox states (Type III).[21] Both inorganic and organic materials have been widely studied and utilized as electrochromic materials. The inorganic materials are mainly consisting of transition metal oxides, such as WO_3[52, 175], Prussian Blue,[3, 53] TiO_2,[192-194], and are usually belonging to Type III. Inorganic ECDs are limited by the inherent disadvantages of the materials: they are chemically unstable, photoactive and brittle and show low coloration efficiency. Comparing to the inorganic electrochromic materials, also organic electrochromic materials have been studied extensively.[18]

The organic electrochromic materials consists of conducting polymers (polypyrrole, polyaniline and polythiophene),[30, 33, 195-197] phthalocyanines,[198] metallopolymers[7, 47, 198]

or viologens. In comparison to the inorganic materials, the organic materials show advantages such as low redox potentials, high coloration efficiency, and fast response time.[7, 199] The organic material can be prepared in different forms and they cover all three types of electrochromic materials that are applied in ECDs. Viologens are good candidates for all three types of electrochromic materials, the methyl viologen (MV) has been utilized to build up ECD of Type I since it is soluble in all of its three forms. Polyviologens on the other hand can be categorized into Type III as they work in solid state. However, the heptyl viologen is classified into Type II, as it turns insoluble when reduced to its radical cation form. In order to increase the performance of viologen materials, especially decrease the response time and lower the reduction potential, a series of viologens has been designed.

Scheme 9. The working principle of electrochromic device **a**) in transmittance and **b**) in reflectance mode.

In the last two decades, P.M Monk and Roger J. Mortimer made a remarkable contribution to the viologen based ECDs research. A series of viologen monomers showing different colors were synthesized and applied in ECDs.[21, 41, 44, 46, 54, 200, 201] Most of them have shown good performances in the ECDs, however, when the viologen monomers were utilized in the ECDs, electrolytes and membranes are needed for the redox response to take place and encapsulation of the electrolyte, will increase the manufacture processes and the cost of the devices. Additionally, as the viologen monomers are usually toxic they don't fulfil the safety demands in the application. Nowadays viologen derivative-based polymers have got increasing attention in the design of the ECDs.[99, 202-208]
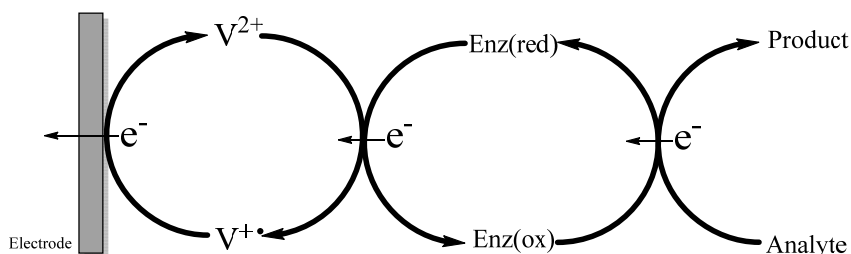
The efficiency of the ECD can also be improved by introducing new functional materials as components in the active material. For example, by introducing TiO_2 into viologens; the efficiency of the ECD can be significantly enhanced.[171, 187, 209] Additionally, in recent years, ECDs based on hybrid materials or composite materials have got much attention and become common,[199]. Viologen materials are also widely studied as a component in other materials, such like ZnO.[210] However, since the mechanism of the electrochromic property of viologen is mainly the same, it will not be discussed in this work.

2.4.2 Sensors and fuel cells

A chemical sensor is a device that can directly measure an unknown analyte.[211] The sensor should be responding continuously and reversibly, without perturbing the sample. A typical sensor electrode consists of a transduction layer and a recognition layer.[211] The transduction layer works as collector for electrons, it usually consists of carbon, Au, Pt and other materials which have high conductivities. The recognition layer should have the ability to react with the analyte, after that the chemically induced change in charge is translated by the transduction layer into an electrical signal, and finally the analyte is detected. Traditionally, the recognition layers in chemical sensors are constructed of varies synthetic functional materials, however, in recent years, biosensors have got word wide attention in which the biological materials (enzyme and bacteria) are introduced to catalyze the chemical reactions. Biological materials have their own advantages, comparing to synthetic materials, such as lower price, available in large amount and extremely good selectivity to the analyte. Even though, the stability and life time of the biological materials may not be as good as for synthetic materials. The electrode which is constructed of biological materials is usually named bioelectrodes, and in recent years, a series of enzymes (or bacteria) are utilized to modify the bioelectrodes.

In order to improve the detection limit, it is important to increase the efficiency of the recognition unit. The electron transfer in the catalyst reaction is in general classified into two types: the Direct Electron Transfer (DET) and the Mediated Electron Transfer (MET). The former is based on the electron tunneling property, which is strongly limited by the materials itself. Usually the active center of biological materials is deeply embedded by the protein, which decreases the DET, leading to quite a low efficiency of the electrode. The MET is accomplished by the aid of mediators, which can facilitate the electron transfer between the recognition layer and the analyte. Mediators consist usually of an organic compound hosting a metal redox site. Common organometallic redox compounds are ferrocene and its derivatives.

Examples of organic redox compounds utilized as mediators are tetrathiafulvalene, Meldola Blue and viologens.[28, 166, 212, 213] In order to work as a mediator, at least two parameters should be fitted: the material should have good redox property and high stability. Additionally, a high solubility of the mediator is demanded. Due to these reasons, viologens have been widely utilized in numerous sensors and biosensors. In comparison to other mediators, there is a significant advantage of viologens, as described above; their redox potential can be adjusted by changing the substituent groups. This property has broadened the application of viologens, as they can be designed for different analytes. Additionally, viologens can be easily attached on varies polymers as pendant groups, which also enhance the electron transfer efficiency between the active centers and the mediators.

Scheme 10. A mediated electron transfer in bioelectrodes using viologens ($V^{2+}/V^{+\cdot}$).

In scheme 10, the mechanism of viologen as a mediator in a biosensor is shown. When the analyte is oxidized by the enzyme, the electron will be transferred to the enzyme from the analyte. The enzyme is then oxidized by the viologen that is reduced to its cation form. Finally the viologen is re-oxidized to its dication form at the electrode surface and is regenerated for the next redox cycle. The sensor will react to the change in electron flow and a signal can be obtained and the analyte can finally be detected.[214, 215] The redox process of viologens lower the electron tunneling potential, which means that the electron transfer rate will be increased, and the performance of the bioelectrodes will be enhanced.

For similar reasons, as in sensing processes mediators are introduced to increase the rate of the reaction in fuel cells. Also here, viologens have been utilized and the mechanism of the mediator in the bio-fuel cell is rather similar to the biosensor already discussed. The growing interest in polyviologens and its composites within the field of sensors and fuel cells is mainly due to the possibilities of device miniaturization. [40, 81, 82, 216].

2.4.3 Further applications

Beside the applications in ECDs and sensors/fuel cells, as one of the most widespread functional materials, viologens have been applied and tested in a variety field of electronics, such like LED,[217] solar cells,[218] and supercapacitors.[219] Additionally, in these years, the viologens have attracted increasing attention in the field of energy storage devices.[220] like redox flow cells, which is a large-scale energy storage device.[221] The application is based on the reductive property of the viologens, with which the viologens can restore the electrons in the radical cation form and even in neutral form. In comparison to traditional inorganic materials, viologens possess advantages such as high solubility, adjustable potential, environment friendly working conditions and lower cost. All of these properties enable viologens to be widely utilized in redox flow batteries in the future.[222] Additionally, viologens are playing an important role in supramolecular chemistry, i.e. in the synthesis of various molecular machines.[34, 223, 224] Beyond that, due to its strong reductive potential, viologens can also be utilized as dopants of other functional materials.[225] These applications are beyond the topic of the thesis and will not be further discussed.

3. Experimental

In order to characterize the viologen materials, electrochemical, spectroscopic and imaging techniques were utilized in this work as main characterization techniques. In this chapter, cyclic voltammetry, chronoamperometry, UV-vis and the FTIR technique will be discussed.

3.1 The electrochemical techniques

In this work, most of the electrochemical experiments were carried out in a three-electrode cell which working principle is shown schematically in Figure 3.1. The cell contains a working electrode (WE), a reference electrode (RE), a counter electrode (CE) and is filled with electrolyte solution containing the monomers. As WE, materials that are inert, has good conductivity and good thermodynamic stability was used, such as glassy carbon, Au, Pt and ITO. The REs should keep a stable potential during the measurement, and in all the experiments here performed, a commercial Ag/AgCl electrode or SHE electrode were utilized. A Pt-wire was utilized as CE due to its good stability. As electrolytes, aqueous or, organic solvents and ionic liquids can all be used together with the viologens. In a three-electrode cell the current is passed between the WE and a CE. The potential of the WE is monitored relative to a RE. The device used to measure the potential difference between the WE and the RE has high input impedance, so that a negligible current is drawn through the RE. During the experiment, the potential is applied between the WE and CE and measured vs the RE, and the current is detected between the WE and CE, By controlling parameters such as time (t), charge (Q) and scan rate (v) varies of electrochemical properties can be measured.
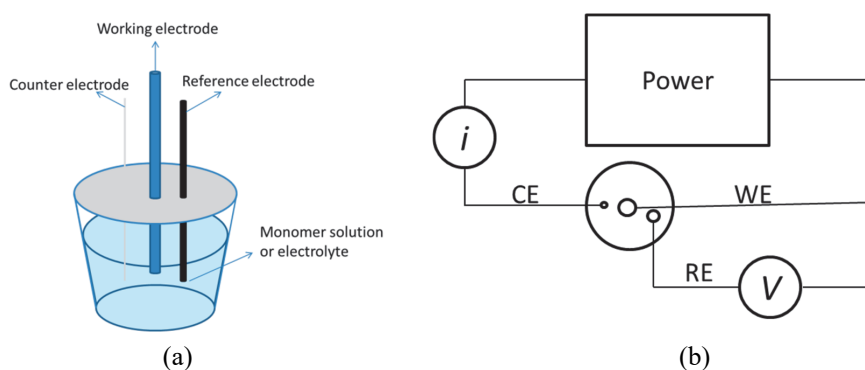

Figure 3.1. (**a**) The three-electrode electrochemical cell, and (**b**) the measuring scheme.

Of all the electrochemical techniques, CV is one of the most versatile and utilized electrochemical techniques. CV is usually the first method applied for detection of redox potentials, determining kinetics of the electron transfer and the diffusion properties.[211] CV has been applied in varies conditions for electrochemical synthesis and analysis. In the electrochemical synthesis, it is easy to detect the monomer or precursor oxidation or reduction potential. Furthermore, after electrosynthesis, CV is usually carried out in a monomer free solution for further characterization i.e. to study the redox reactions for the formed material. By changing the scan direction; the reversibility of the material can be measured, by repeating the CV continuously; the stability of the material can be characterized.

The working principle of CV is shown in Figure 3.2. At a certain starting potential ($E_{initial}$) a continuously higher potential is applied at a certain rate ν between the two electrodes until a certain potential value (E_{final}) is reached. The potential scan can be applied in either positive or negative direction, which will lead to an oxidation or a reduction reaction, respectively. If the experiment ends at E_{final} the technique is named linear sweep voltammetry (LSV). After achieving the highest (lowest) end potential, the potential will be reversed back to its initial value, and one CV cycle is completed. During the CV sweep, the current resulting from the reaction is measured, and the *I* vs. *E* plot is named a cyclic voltammogram, which is a time-dependent function. In Figure 3.2b, a theoretical reversible redox process in a CV is shown. It is assumes that only one reductant is present in the solution. The scan is applied from 0 V (vs Ag/AgCl) and is increased until the characteristic potential for the oxidation process of the studied material is achieved; an anodic current peak is formed. The peak current (I_{pa}) can be obtained when the peak value (E_{pa}) is achieved, after that the current will drop down with increasing potential. The reason is due to that the reaction is limited by the diffusion, which means the reductant surrounding the working electrode surface is consumed, and the diffusion of the same is not fast enough to maintain the reaction. The depletion causes the current decrease even if the potential is continuously increasing. The sweep is reversed when the final potential is reached, and at the same potential, the oxidants which are formed during the forward half-cycle are reversible reduced. The cathodic current peak is formed correspondingly. With repeating cycles, the material will be synthesized.
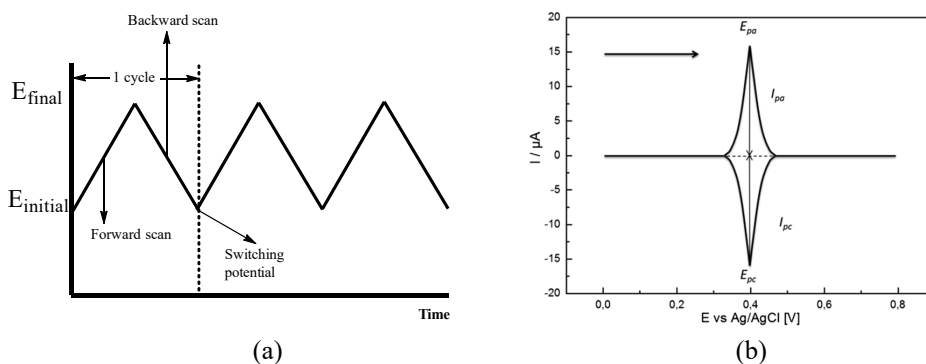
	(a)	(b)

Figure 3.2. Potential-time signals in cyclic voltammetric experiment (**a**), and idealized cyclic voltammogram showing the redox process of a hypothetical redox couple (**b**).

Another common electrochemical technique is chronoamperometry (CA), which has also been utilized in this work as polymerization and characterization technique. In Figure 3.3, the typical CA process is shown. Similar as the CV, the CA is also a time-dependent function.
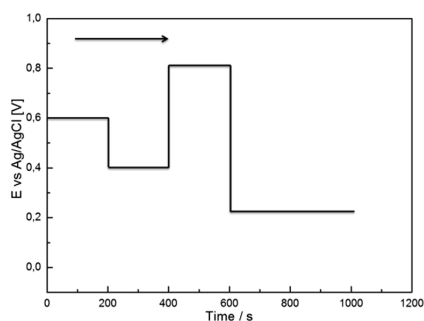

Figure 3.3. A chronoamperometry measurement with four different potential levels

In a CA measurement, one or more potential levels can be applied on the WE. In contrast to CV, the changes in potential are not continuous but can be applied directly from one value to another. Additionally, the time at each potential can be set at any particular values for different measurements. Comparing to the CV, the advantage of CA in electrochemical synthesis is that it is easier to control the amount of charge (Q) used during the electropolymerization, and indirectly the thickness of the resulted adsorbed films, especially in the synthesis of conducting polymers.

The CA is also widely utilized in electrochemical analysis, especially in *in situ* measurements when combined with other techniques. This technique is more efficient, especially for redox polymers, where one wants to analyze the difference in material properties at precise potentials. Additionally, as the redox reaction occurring at the

electrode surface is usually diffusion controlled, CA can be used for determining the diffusion coefficient of the redox material according to the Cottrell equation (5).

$$i(t) = nFACD^{1/2}/(\pi t)^{1/2} \tag{5}$$

Where: i is current (A); n is number of electrons; F is Faraday constant (C mol^{-1}); A is the surface area (cm^2); C is the concentration (unit); D is the diffusion coefficient (cm^2 s^{-1}) and t is time (s). In this work, the CA technique was utilized to measure the effect of different anions on the properties of polyviologens (**Paper II**).

3.2 Spectroscopic techniques

Spectroscopic techniques are widely utilized in the characterization of materials. The measurements study the interaction between matter and electromagnetic radiation which can be determined through absorption, transmission and reflection. Depending on the energy level of the electromagnetic spectrum, shown in Figure 3.4, the samples can be measured focusing on different purposes. For example, at high energy, the X-rays can be used to detect the elements of the sample, and at lower energy, the structure of the sample can be analyzed by Infrared spectroscopy. In order to measure and analyse the materials, a series of different instrumentation have been design based on the different electromagnetic ranges.
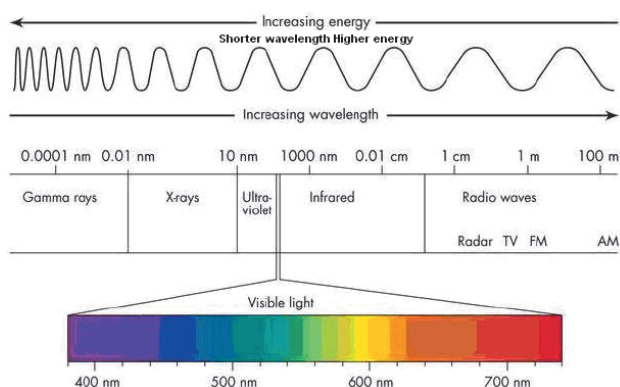

Figure 3.4. Electromagnetic spectrum showing its wavelength and energy range.

3.2.1 *In situ* UV-vis spectroscopy

The combination of electrochemical and spectroscopic methods has been applied from last century in order to investigate the properties of the materials during an electrochemical process. With the combination, the electrochemical properties, especially the redox property can be successfully measured. Different electrochemical methods and

varies spectroscopic instrumentation have been combined together for many different application. *In situ* UV-vis (ultraviolet-visible) spectroscopy is one of the most utilized methods in the characterization of varies organic monomers and polymers. In the previous part, the redox properties of the viologens have been described from several aspects, and discussed in **Paper I** and **Paper II**. The common methods for characterizing the redox processes are CV and UV-vis spectroscopy. As the absorptions of viologens in their different redox forms are characteristic, *in situ* UV-vis spectroscopy is very useful to determine redox states and redox induced changes in viologens and polyviologens.

The optically transparent electrode (OTE) is the most central part in the *in situ* UV-vis measurement setup. Their transmittance is the critical parameter in order not to limit the light passing through to the electrode surface. However, while the absorptions of the materials are controlled by the electrochemical measurement, the conductivity of the OTE is also very important. Usually the OTEs consist of glass, quartz or metal micromesh. In order to increase their conductivity (for glass and quartz based OTEs), a metal (Au, Pt) or semiconductor (indium tin oxide/tin oxide) layer of a certain thickness is deposited on the substrates. In Figure 3.5 (a), the electrochemical cell which was used for the *in situ* UV-vis spectroscopic measurement is shown. The ITO glass is placed in the cell as working electrode, so that the electromagnetic beam can pass. A Pt wire works as a counter electrode and a commercial Ag/AgCl electrode is used as reference electrode. They are placed on the sides of the ITO glass so that the UV-vis beam will have a clear passage. In this work, the polyviologen films were firstly synthesized by electrochemical methods (CV or at constant potential) in an electrolyte solution containing the monomer. After film formation the WE was rinsed with electrolyte and placed in a cuvette filled with monomer free electrolyte solution. By comparing the UV-vis absorption before and after the electrochemical polymerization, new absorbance bands due to the formed material can be obtained. These together with CV data can furthermore be used for calculation of the band gaps of the different polyviologens.
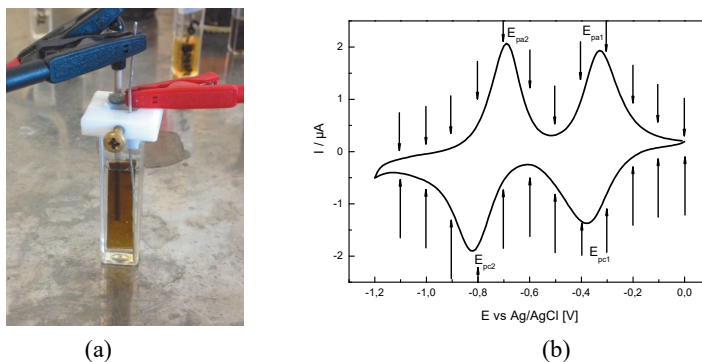

(a)	(b)

Figure 3.5. (**a**) Electrochemical cell used for *in situ* UV-vis measurements (**b**) the applied potentials during the *in situ* measurements shown by arrows.

After electropolymerization, the formed polyviologen film was characterized by UV-vis during staircase increasing constant potential. As shown in Figure 3.5b, the potential is increased by 0.1 V for every staircase applied on the electrode for a certain time (from several seconds to several minutes) between 0 and -1.1V. After this the scan is reversed and the material studied on the backward scan. In the UV-vis experiments, the UV-vis absorptions of the polyviologens films were recorded when a stable current value was achieved. By analysis of the absorption variations at different applied potential, the redox properties of the viologen materials can be analyzed. Furthermore, by comparison of the shifts in absorbance, changes in the structure of varies viologen material can be studied. Additionally, the new bands which are formed during potential application indicate the different specific redox forms of the viologen units (**Paper I**, **II**, and **IV**).

3.2.2 FTIR spectroscopy

Fourier transform infrared spectroscopy (FTIR) was used in this work to verify the structure of the electrochemically synthesized polyviologen films. As shown above in Fig 3.3a, the energy of the IR source is weaker than that used in the UV-vis. In the IR range the molecular vibrations which are caused by interaction between the sample and the IR light source can be studied and provide information of the structure of the materials, which is particularly useful in the characterization for different organic materials. There are three types of vibrations: bending, stretching and rotating, and each of them contain different sub types. Based on the frequencies, the IR spectrum is usually divided into three regions: near-infrared region (from 13000 to 4000 cm^{-1}), mid-infrared region (from 4000 to 400 cm^{-1}) and far-infrared region (from 400 to 100 cm^{-1}). The intensities of the bands in the near infrared region are much weaker than those in the mid-infrared region, and the far-infrared regions are usually utilized for the characterization of the compounds which contain heavy metals, the molecular torsions and the crystal lattice vibrations.[226] Due to these reasons, the application of IR spectroscopy is mainly focused on the mid-infrared region. A mid-infrared spectrum with the different vibration-regions is outlined in Figure 3.6 below.
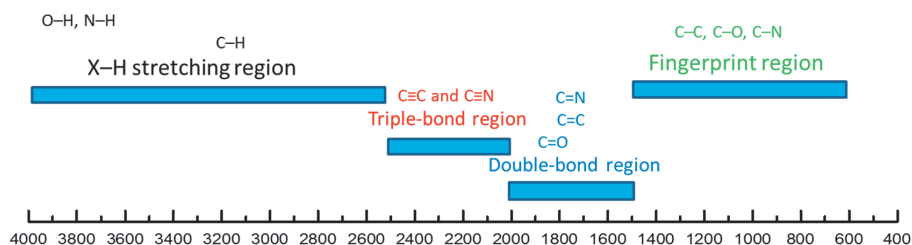

Figure 3.6. The mid-infrared spectrum

The mid-infrared spectrum can be divided into four regions: 1), the X-H stretching region (4000-2500 cm^{-1}); 2), the triple-bond region (2500-2000 cm^{-1}); 3), the double-bond region (2000-1500 cm^{-1}); and 4), the fingerprint region (1500-600 cm^{-1}). It should be pointed out that the vibrations of each bonds are not constant, which means they can be affected by several parameters, such as skeleton, neighboring molecule or atoms, the conjugated structure and so on. The complexity of the 1500 to 600 cm^{-1} region makes it difficult to assign all the absorption bands, and because of the unique patterns found here, it is often called the fingerprint region.

In this work, FTIR was utilized in the characterization of both the monomers and the resulting viologen materials. By comparing the absorption value in the triple-bond regions, the electrochemical synthesis of the viologen materials can be followed, due to decreasing absorption of C≡N bonds and increasing intensity of C=N. Furthermore, the different absorption bands and the shift of the band indicate changes in the structures of the polymers. The details will be discussed in Part 4.

3.3   Microscopic techniques

In order to characterize the morphology and coverage of the viologen films, microscopic (imaging) techniques were introduced for the characterizations. In this work, Atomic Force Microscopy (AFM) and Scanning Electron Microscopy (SEM) were applied to measure the surface morphology of the films. AFM is one of the most utilized techniques to study the surface with high resolution and accuracy. Generally, the critical parts of the AFM equipment consist of a cantilever and a laser reflection system. A sharp tip is placed at the end of cantilever, and the laser spot is concentrated on the tip. When the tip is directed on the sample, at a certain short distance from the surface, the force between the end of the tip and the sample surface cause a deflection, which can be detected by the laser reflection system. During the measurement, the tip moves on the top of the sample surface within a certain area, and the signals of the force can be obtained by the laser reflection. By calculation and computer analysis, the AFM image of the surface of the samples can be obtained. It should be mentioned that the quality of the AFM image is strongly affected by the size of the tip, by adjusting the tips, the samples in different conditions can be measured. For example, the tip with higher stiffness of 40 N/m is suitable for the solid sample in tapping mode. Tips with lower stiffness of 5 N/m is more useful for the measurement of soft materials or particles with low adhesion to the surface. Additionally, the tips can be further modified for special applications (e.g. conductive AFM)

Unlike other surface characterization techniques, AFM has its own advantages, such as mild measurement condition, no special preparations for the samples; the sample can be conducting or insulating, and the ability to measure in X, Y and Z direction. However, the main disadvantage of AFM is the size of the measurement area usually limited to 100 μm, due to that the AFM need to scan the surface of a sample, and a large area means increase in measurement time.[227] Furthermore, since AFM can detect the samples in 3-dimensions, it is very useful to measure the thicknesses of the films. Of the same reason, AFM was also utilized to measure the different thickness of the self-assembly formed monolayers, and the results are shown and discussed in part 4.

In this work, viologen materials were also studied by SEM for their surface characterization. Especially in the SAM work, with the support of SEM, the ordered structure of polyviologens was successfully analyzed.

3.4 Other techniques

There are many other types of techniques and methods applied to analyze the structures and properties of polyviologens. For the self-assembly formed monolayer, the surface property was measured using the contact angle, which can give information on the coverage of the monolayer on to the electrode surface. The Polarization modulation infrared reflection adsorption spectroscopy (PM‐IRRAS) was also utilized to characterize the SAM layers due to its high surface sensitivity. Additionally, the effect of H_2O and CO_2 can be almost eliminated, which is due to the independency of the isotropic adsorption from gas or water. By the analysis of Raman spectroscopy, the reduction of the graphene oxide in the composite film could be shown. Furthermore, by using the electrochemical impendence spectroscopy (EIS) technique, the resistance (conductivity) of the composited film can be roughly calculated. The result of these measurements will be discussed later in Part 4.

4. Result and discussion

4.1 Electrochemical synthesis

The aim of this work is to study the electrochemical properties of viologens materials, especially polyviologens. Electrochemical synthesis of various polyviologen films from different CP-monomers, synthesized in the group, was performed (structures shown in Scheme 5).

Polyviologens have been electrochemically synthesized by two different methods, as described in the experimental part: by CV or by CA. In Figure 4.1, characteristic cyclic voltammograms of the electrochemical polymerization of a CP-monomer in aqueous solution is shown. The polymerization is carried out by CV during 20 cycles; the first cycle is shown as an insert in Figure 4.1. When a negative potential is applied on the electrode, the current is quite stable at the beginning. However, when the potential reaches approx. -0.7 V, a sharp reduction peak is formed. The peak is due to formation of the viologen units, which means two 4-cyanopyridium moieties are reduced to the neutral form by removal of two cyano groups. In the backward scan a sharp re-oxidation peak is obtained at -0.5 V, which is from the re-oxidation of the viologen to its dication form. During continuous scans, the current peaks which are formed at approx. -0.7 V and -0.5 V are shifted to -0.9 V and -0.3 V correspondingly, simultaneously as they start to decrease. The process is described as a result of formation of viologen dimers, oligomers and polymers followed by deposition at the electrode surface. Additionally a weak reduction peak is formed at approx. -0.55 V, and another re-oxidation peak is formed at approx. -0.8 V. These new peaks are due to the redox response from the polyviologens which has been already formed at the surface of the electrode. The result is shown in **Paper I**.
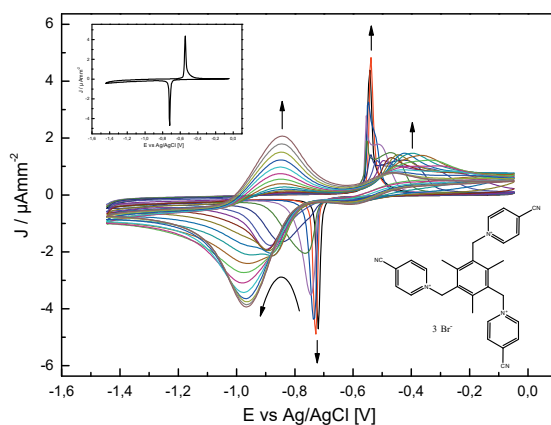

Figure 4.1. Cyclic voltammograms from electrochemical polymerization of the 5mM monomer TCP in 0.1 M KCl aqueous solution at a scan rate 50 mV/s on the GC-electrode for 20 cycles. (The inserted figure in top-left shows the first cycle)

The electrochemical synthesis of polyviologens is not only carried out from the single monomers, but also using different monomer structures for the formation of copolymer films. As described above, the viologen unit can be formed by coupling of two cyanopyridine moieties, which can be positioned at different monomers. In Figure 4.2 the electrochemical synthesis of a copolyviologen is shown, which is formed between two different monomers (TCP and LCP). The electrochemical synthesis process is similar to the one shown in Figure 4.1; the peaks are overlapped by those from the polymerization of TCP. However, it should be noticed that there are two new current peaks formed at approx. -0.5 V and -0.35 V (shown with dashed arrows in Figure 4.2.). These current peaks are rising due to the introduction of a LCP into the polymerization solution forming a copolymer with TCP. The peak at -0.5 V indicates that the LCP is successfully coupled with the TCP, and the peak at -0.35 V indicate that the viologen is re-oxided to its dicationic form. During continuous cycling, the reduction peaks shift to more negative potentials while the oxidation peaks shift to more positive potentials, due to the formation of the polyviologen at the electrode surface. The work is shown in **Paper I**.
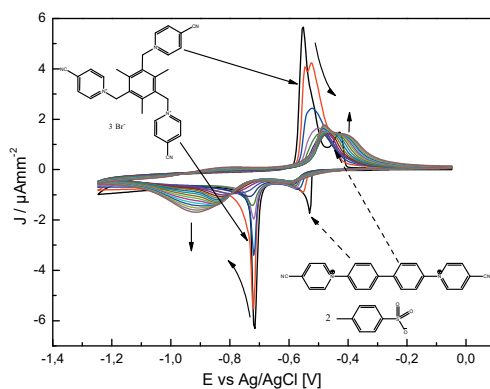

Figure 4.2. Cyclic voltammograms of the electrochemical polymerization of the monomer TCP (5 mM) and LCP (2 mM) in 0.1 M KCl solution in the potential range 0 to -1.2 V at the scan rate 50 mV/s for 20 cycles.

The electrochemical synthesis of polyviologen can also be carried out on a modified electrode of special design. In this work, a new linear polyviologen is successfully synthesized on a SAM modified electrode (**Paper III**). Firstly, the cysteamine (SNH_2) is formed on the plasma cleaned Au electrode surface through SAM method, thereafter a precursor (SCNCP, structure shown in scheme 5) having an isothiocyanate group as the head group and the cyanopyridine groups as the tail group is introduced. By the reaction between the isothiocyanate group and the amine group, the precursor is linked at the SAM modified electrode, the cyanopyridine group will be utilized for viologen unit formation in the following electrochemical polymerization process. In

Figure 4.3, the electrochemical polymerization of LCP at a SNH_2-SCNCP modified electrode is shown.

Similarly as for other electrochemical synthesis processes, the reduction peak at approx. -0.45 V indicates the formation of the viologen unit, and the peak at approx. -0.3 V is due to discharging of the viologen back to its dication form. The enlarged selected cycles shown as an insert in Figure 4.3 show the progress of a film formation. However, comparing to the electrochemical synthesis in previous CVs, the shifts of the peaks and the formation of the new peaks are not as clear. This can partly be explained by that the electrode has been modified by SNH_2 and SCNCP before the polymerization and the response of the redox reaction of the viologen is therefore strongly overlapped by the background current.
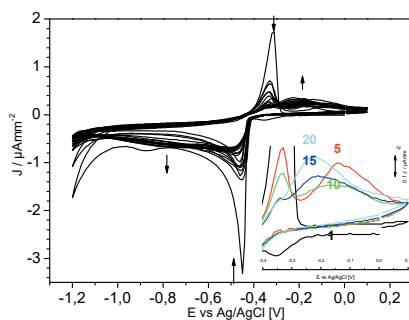

Figure 4.3. Cyclic voltammograms of the electrochemical polymerization of the 2 mM LCP on SNH_2-SCNCP primed electrode in 0.1 M KCl solution in the potential range 0 to -1.2 V for 20 cycles at scan rate 10 mV/s.

The electrochemical synthesis of polyviologens, using varies monomer structures, has been successfully performed in aqueous solutions. However, even the GO can be successfully dissolved into deionized water, it will start to aggregate after introduction of small ions into the solution. It is assumed that the ions will strongly effect on the charge distribution of the GO, leading to aggregation, which will hinder its incorporation into the PV during electrochemical polymerization. In order to synthesize a new composite film, consisting of viologens and reduced graphene oxide, the electrochemical polymerization was switched from aqueous media to ionic liquids (ILs) (**Paper IV**). The advantages of ILs have been described above in part 2.3, such as the large electrochemical window, it can be seen from Figure 4.4 that the potential for electropolymerization has been extended to -1.6 V, which is much broader than for aqueous solution. In order to solve the GO into the IL, the aqueous GO solution was firstly mixed with IL. Directly upon mixing a phase separation could be observed but after constant stirring a homogeneous solution was obtained. After stirring the mixture was distilled using a rotary evaporator under 2 mbar and 45 °C for 4 h and furthermore

dried in vacuum oven at 10 mbar and 45 °C for 4 h. After that, the TCP monomer and graphene oxide can be mixed in IL without any aggregation.

The CV of the electrochemical polymerization of the TCP and GO in ionic liquid is shown in Figure 4.4. The first cycle is shown as an insert. In the first cycle there are two reduction peaks formed at approx. -0.4 V and -0.6 V. The first one is from the formation of the viologen unit; a corresponding oxidation peak of the same can be found at -0.38 V. The second current peak is from reduction of graphene oxide, there is no corresponding oxidation observed in the reverse cycle. In the following CVs, the current peaks disappear quite quickly, which is due to that the monomer and graphene oxide nearby the electrode surface has already been reduced. However, the formation of the new reduction and oxidation peaks indicate a successful formation of the viologen film onto the electrode surface. This result is described in **Paper IV**.
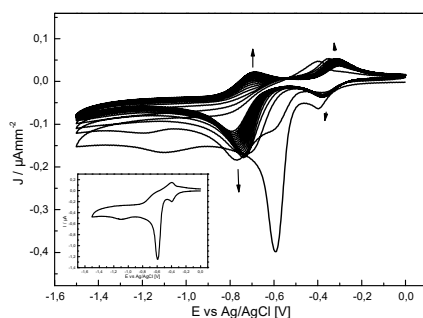

Figure 4.4. Cyclic voltammograms of the electrochemical polymerization of the TCP and graphene oxide in ionic liquid BMIMBF$_4$ in the potential range 0 to -1.6 V with the scan rate 20 mV/s.

As described in part 3.1, CA is also widely utilized for electrochemical polymerization of polyviologens after the reduction potential of the monomer or precursor is detected. It is easier to control the charge during the electropolymerization by CA, by which the thickness of the film can be estimated. The film thickness is very important for the comparison of different polyviologen films, for example, when the influence of different sized anions on film formation of polyviologens is compared. In Figure 4.5a a typical CA curve, obtained upon electropolymerization of monomer T2, is shown. The CA curve of an electrochemical polymerization of T1 is shown in Figure 4.5b, which differs from a regular CA curve. The current oscillates intensively at the beginning of the polymerization process, and this tendency continues throughout the whole experiment. Such oscillations are typical for systems that are far from thermodynamic equilibrium. The reason for this phenomenon was not studied in more detail as in this work the CV technique was mostly used for the electropolymerization of PV films. In Eeva Kopperoinen's master thesis oscillative electrochemical reactions were studied for a three branched CP-monomer.[228] During electropolymerization the

frequency and duration of the oscillation were found to be depended on monomer concentration and rotation speed of the electrode. Also the polymerization potential and electrolyte utilized in the polymerization had an influence on the frequency of the oscillation. If the rotation speed or concentration was increased, the frequency of the oscillation decreased why it was assumed that the oscillation was caused due to slow diffusion of the monomer to the electrode. Also the roughness of the electrode affected the oscillation, the rougher the electrode, less oscillations could be observed.
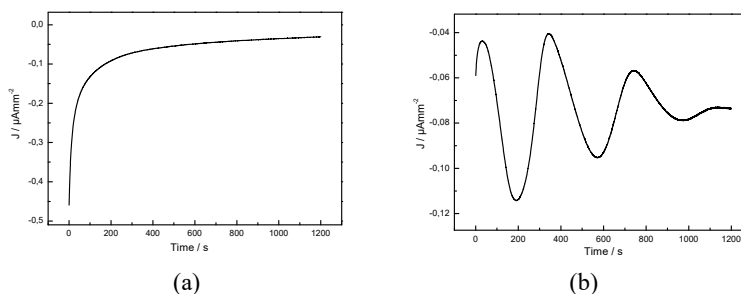

(a) (b)

Figure 4.5. Chronoamperometry of the (**a**) electrochemical polymerization of T2 and (**b**) electrochemical polymerization of T1.

4.2 Electrochemical characterization

The redox response of two different polyviologens is shown in Figure 4.6 below, and the structures of the monomers are inserted in the figures. The CVs are carried out at different scan rates varying from 10 mV/s to 100 mV/s in monomer free electrolyte solution. From the redox response of the polyviologen films it can be observed that the peak currents are increasing with the scan rates. As an example, in Figure 4.6a, the first reduction and oxidation couple (which are marked as R1 and O1) at approx. -0.39 V and -0.32 V, is due to the switching of the viologen from its dication form to radical cation form and vice versa. The reduction/oxidation peaks from the second redox couple (which are marked as R2 and O2) are at approx. -0.82 V and -0.68 V and originates from the switch of the viologen radical cation form to the neutral form. The changes of peak currents with different scan rates for polyT1 are shown in Figure 4.7.

In Figure 4.6b, the redox response of another polyviologen (TPV) is shown. The structure of the monomer is similar to monomer T1, however, the properties of the polymer differs from that obtained for PolyT1. The first redox couple of TPV is less reversible in comparison to the second one. There are many different parameters which will lead to this effect, such as lower redox activity due to steric hindrance in the structure of the films, the electrolyte or the thickness of the film. In this case it can

mostly be explained by difference in film thickness (observed in SEM measurements, which is about 600 nm in here) causing the lower current values.
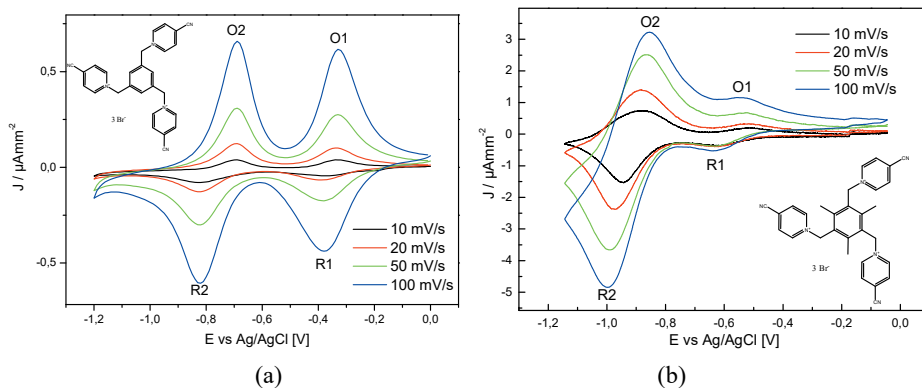

Figure 4.6. Cyclic voltammograms of two different polyviologen films in monomer-free solution 0.1 M Na_2SO_4 (**a**) PolyT1 and (**b**) TPV.

The influence of scan rate on the redox response is shown in Figure 4.7 below. The peak currents of the two redox couples were picked from Figure 4.6a. The oxidation currents increase with the scan rate but not linearly. However, neither the Randles-Sevcik nor the ideal Nernstian behavior is fully valid for redox polymers. The ideal behavior is valid just for conditions when using relatively slow scan rates, and for an adsorbed layer if the electron transfer is fast enough. The charge transfer in a network of a redox polymer is more complicated and the diffusion control may not be the dominating parameter. Furthermore, the peak-to-peak separation for the PolyT1 film was $\Delta E_1 = 70$ mV and $\Delta E_2 = 140$ mV which means that the electron transfer in the polyviologen films is quasi reversible. According to Bruinink et al. the film deposition of viologen material takes place due to a radical salt formation. In cases when the potential scan is reversed directly after the first reduction the changes involved in the cathodic (Q_c) and anodic (Q_a) scans approach unity. Extending the scan over the second peak introduces aging products in the film that might cause crystallization which influences the electrochemical response. Additionally, viologen dimerization takes place in the film as will be discussed later in the UV-vis section, interactions that influence the peak-to-peak separation as well. The slight asymmetry in the broadness of the first redox couple might be due to that the viologen was switched into its conductive phase from the non-conducting phase when it is reduced to the radical cation form. In the reverse scan, the film was brought from its conducting phase to its non-conducting phase.
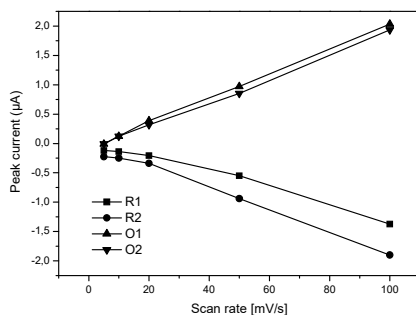
Figure 4.7. The peak currents of the reduction/oxidation for polyT1 the two redox pairs vs. the scan rates.

The influence of the different anions on the properties of polyviologen films has been studied in aqueous solutions.[2, 169, 178-182] It can be assumed that the same reactions take place to some extent also in the solid phase of a viologen film. In this work, two polyviologens were electrochemically synthesized in monomer solutions which were prepared with three different electrolytes: KCl, Na_2SO_4 and NaPSS. However, T2 could not be electrochemically polymerized when NaPSS was used as electrolyte, in total 5 films are synthesized and compared. All of them are characterized in three different electrolytes in the potential range 0 to -1.2 V in order to study the anion induced changes in the polymer redox reactions. The results are shown in Figure 4.8, a-e show the redox responses of PolyT1 and PolyT2 when polymerized in presence of KCl, Na_2SO_4 or NaPSS. The f-j shows the curves of decay in potential at open circuit displayed as potential vs. time after that the films were charged at potentials corresponding to the neutral form of the polymer (approx. -0.8 V).

Of all of the films, only PolyT1 which was made and cycled in KCl shows a reversible two step redox response of approximately equal current intensity from both redox couples. Figure 4.8a shows that when the electrolyte is switched to Na_2SO_4 or NaPSS the current from the radical cation ($2PV^{+\bullet}$) is decreased meanwhile the current from the second reduction leading to the neutral form (PV°) is dominating. There are many parameters which can cause this effect, such as the size, mobility and valence number of the anion, the interactions between the viologen unit and the anion and the structure of the polymer material. All the aforementioned parameters might influence the viologens radical salt formation which might lead to crystallization or recrystallization in the film upon cycling. These properties influences further the rate and presence of the dis- ($2PV^{+\bullet} \rightarrow PV^{2+} + PV^{\bullet}$) and comproportionation reactions ($PV^{\circ} + PV^{2+} \rightarrow 2PV^{+\bullet}$) taking place in the film (**Paper II**).

By comparing the redox responses of the films, it should be noticed that the highest currents were always obtained if the films were synthesized and cycled in the same electrolyte. Figure 4.8b shows the redox response of the film made in presence of Na_2SO_4. When cycling the film in a divalent anion containing electrolyte (like SO_4^{2-}) the radical formation takes place at slightly more negative potentials. From Figures 4.8 a-c one can notice that independently what electrolyte was used for film preparation, cycling in Na_2SO_4 always shows the lowest peak potential at the first redox couple. In KCl and NaPSS the values of the peak potentials almost match indicating that it is more the divalency and not the size of anion that is important in the first one-electron transfer step (V^0 to $V^{+\bullet}$). The NaPSS containing film showed a broad, potential shifted second reduction peak preceded by a pre-peak (Figure 4.8 c). The slight overpotential needed to obtain the neutral state is caused by the almost stationary counter ion, PSS^-. Other factors that might cause distortion of the voltammogram is the dimerization of the radical viologen cation, also referred to π-dimerization which can be seen in the UV-vis spectra as an absorbance at around 560 nm and second one around 900 nm, shown in Figure 4.9 later on in the UV-vis Part (in section 4.3).

In the E vs t curves of the PolyT1 films a very fast potential decay can initially be seen until reaching the potential region for the radical form at around -0.4 V (Figure 4.8 f and g). The stability of the radical cation varies with the type of anion and is at least stable with SO_4^{2-} when films are made in presence of either Cl^- or SO_4^{2-}. In the case of films made in presence of PSS^- the trend is changing, here the radical form is stable in the case of cycling in Cl^- or SO_4^{2-}. The two-step plateau voltage near -0.4 and -0.8 V agree well with the redox potential of the films shown in Figure 4.6a. These results indicate that the charge diffusion for the second redox reaction of PolyT1 ($PV^\bullet$ to $2PV^{+\bullet}$) was much faster than that of the first reaction. PolyT2 shows a very weak redox response from the radical form in all three electrolytes. Nevertheless, upon open circuit measurements after charging, all the films finally relax towards a potential representing the state of the radical cation and forms a constant potential plateau.
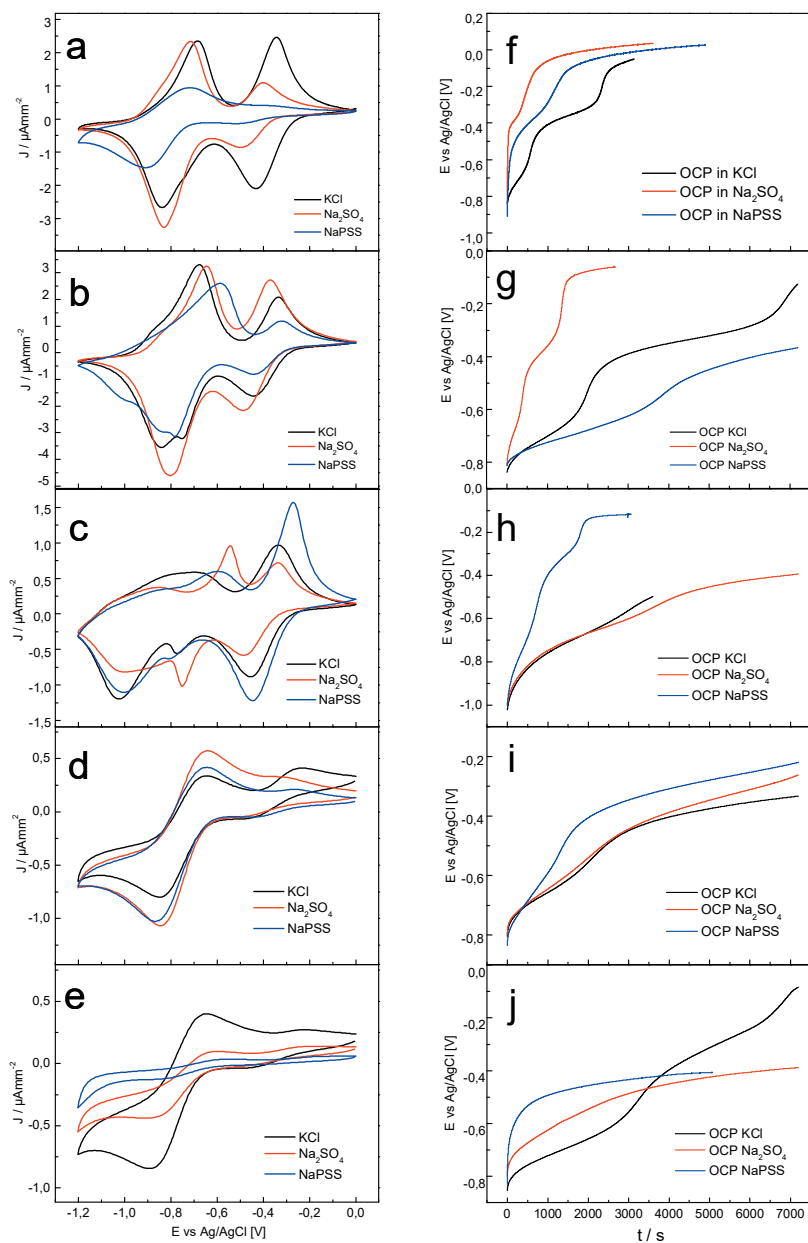
Figure 4.8. a-e show the CV:s of KCl, Na$_2$SO$_4$ or NaPSS prepared PolyT1 and PolyT2 in each of the three different electrolytes at a scan rate 50 mV/s, **a**) PolyT1(KCl), **b**) PolyT1(Na$_2$SO$_4$), **c**) PolyT1(NaPSS), **d**) PolyT2(KCl), **e**) PolyT2 (Na$_2$SO$_4$). **f-j** show the curves of decay in potential at open circuit displayed as potential vs time, **f**) PolyT1(KCl), **g**) PolyT1(Na$_2$SO$_4$), **h**) PolyT1(NaPSS), **i**) PolyT2(KCl), **j**) PolyT2(Na$_2$SO$_4$).

There is always a strong intermolecular interaction between the viologen cation radicals which gives rise to the comproportionation. The type of anion does not seem

to have the same influence on the redox response in PolyT2 as in PolyT1. It has also to be mentioned that in case of using NaPSS as electrolyte the film formation of polyT2 was poor and such films could not be included for the redox and discharging studies. The stable radical form of PolyT2 could be utilized in a process where a film needs to be reversibly conducting for some time. Similar systems containing bulky anions has been built from poly(ethylenedioxy thiophene), PEDOT-PSS, with the drawback that it stays in its conducting form and is not able to switch between non conducting-conducting states. In general conducting polymers undergo a conducting-non conducting redox switching but very few of them display a stable radical/polaron state.

4.3 UV-vis spectroscopy

In situ UV-vis measurements were carried out as described in part 3.2.1. The absorptions of two different polyviologens (PolyT1 and PolyT2) are shown in Figure 4.9, respectively. The inserted graph shows the peak values of each band and their changes with the applied potentials. At the beginning, the absorbance start to slowly increase until the potential -0.4 V is reached. Three broad absorbance bands can be observed with peak maximum at approx. 390, 590 and 920 nm. The absorbance band at 390 nm is increasing throughout the hole potential scan but the other two absorbance bands start to decrease after a potential of -0.7 V has been reached. It has been reported that the absorbance band at 590 nm is due to formation of the viologen radical cation. As discussed in part 4.2, upon reduction of polyviologen the radical cation is firstly formed. However, after the second reduction peak, the viologen radical will be further reduced to its neutral form, why the absorbance from the radical cation starts to decrease. As the band at 390 nm rises from the absorbance of the neutral form of viologen, it will can keep increasing with the applied potentials.

By comparing the two UV-vis spectra, it can be noticed that the absorbance band at 920 nm is unique for PolyT1. This band is corresponding to viologen dimers that are formed due to the response from interaction of closely spaced viologen units. Of the same reason, a second absorbance band should appear at around 560 nm. However, in this case it is overlapped by the strong band at 590 nm from the viologen radical. This dimer band cannot be observed in the spectra of PolyT2, which is due to the different monomer structures, T2 has a longer substituent chain comparing to monomer T1. After polymerization the viologen units are isolated from each other, under this condition, dimer-type interactions between the viologen units are less probable. Furthermore, when comparing the absorbance bands of the two polymers, a shift of the band at around 600 nm in PolyT2 appears, which indicates a lower dimer type

contribution. The degree of dimerization is reported to increase with the hydrophobicity of the molecule or the substituent on the bipyridine ring. This might partly explain why the absorbance of the radical cation form in PolyT2 is higher than that in PolyT1. The Changes observed in the UV-vis are reversible, during the backward scan the viologen was re-oxidized from neutral form to its radical cation and finally to its dication form.
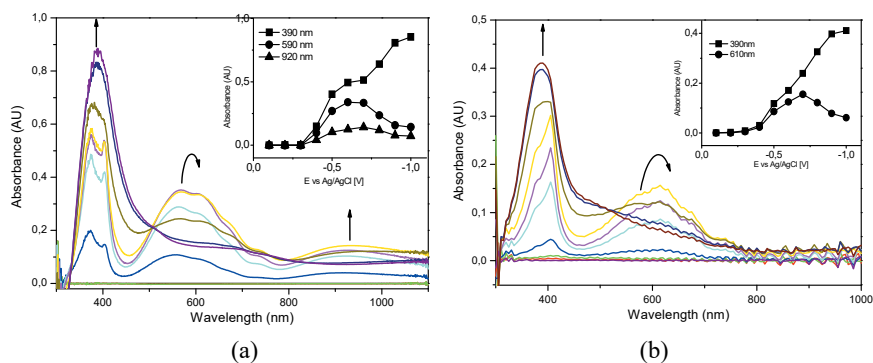

Figure 4.9. The *in situ* UV-vis spectra of (**a**) PolyT1 and (**b**) PolyT2 in the potential range from -0.1 to -1.0 V. The peak values of the absorbance bands at 390, 590 and 920 nm corresponding to the applied potentials are shown as insert in the top right of the figures (**Paper II**).

A clear advantage of the *in situ* UV-vis spectra is the possibility of detecting the different states of viologens during redox reactions. In this work, branched cyanopyridine films were formed and characterized by UV-vis spectroscopy. In Figure 4.10, the UV-vis spectra of the differently branched viologen films in their radical cation forms are shown (monomer structures shown in Scheme 5).

All of the polyviologens studied show a absorbance response at 400 and 600 nm. However, the absorbances at around 900 nm are observed only for the TPV and the PolyT1 indicating dimer formation of the radical cation in the polymers. For the rest of the branched polymers, the absorbances at 900 nm cannot be observed, which can be explained by that their cavities are too large for dimer formation. Furthermore, the absorbance bands at 400 and 600 nm are split into two bands, observed especially for TPV and PolyT1. It is assumed that these absorbance bands are from the viologen group (380 nm) and phenyl group (410 nm), respectively. In TPV and PolyT1, the viologen groups are present in a larger extent, thus the absorbance at 380 nm is dominating the spectrum. However, in the other polymers studied, the structure of the monomers differ, they contain less pyridine groups why the absorbance at 380 nm becomes relatively weak. The band at 600 nm also consists of two parts, containing contribution from both phenyl and viologen groups. Variations in internal vibration

intensities within this band shows the different proportions of viologen groups and phenyl groups present in the polymer structures. The TPV was studied in **Paper I** and **IV**, the PolyT1 and PolyT2 were studied in **Paper II**, the PolyCSBCP will be shown in the further research, and the CoPV was studied in **Paper I** also.
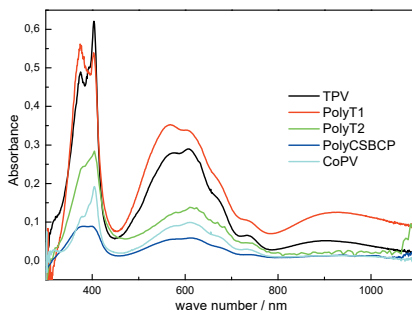

Figure 4.10. *In situ* UV-vis spectra of the different polyviologens/copolyviologen films in their radical cation form

4.4 FTIR

In this work, FTIR was mainly used to characterize and compare the differences in structures of the viologen materials (monomers and films). Some specific bands which are closely related to viologen materials should be pointed out: firstly, the absorbance at around 2235 cm^{-1}, which is due to the vibration of the C≡N bonds. As the cyano groups in the monomer are removed during the polymerization process, this C≡N band should weaken after electropolymerization. In all of the structures studied the decrease of the C≡N bands can be observed, which indicated that all of the viologen materials were successfully synthesized. Secondly, the band at around 1640 cm^{-1} is due to the vibration of the C=N, which is a strong evidence for the presence of pyridines or viologen units. In this work, almost all the pyridine groups in the monomers which have been utilized for the electrochemical polymerization are bond to a benzyl group (except for LCP). The N-CH stretch at approx. 1210 cm^{-1}, is also important when characterizing viologen materials. On the other hand, the presence of phenyl groups can cause similar vibrations, especially the vibration of C=C and CH$_{ring}$ in phenyl groups are overlapping the vibration from C=N and CH$_{ring}$ in viologens, which increased the difficulty in the analysis of the FTIR spectra.

In Figure 4.11b, it should be notice that the C≡N band around 2230 cm^{-1}, can still be seen in the spectra which indicates there are still cyanopyridine groups left after the polymerization, probably at the endings of the polymer chains. Furthermore, in the FTIR spectra of the SCNCP-polyLCP film, two peaks are seen at 2230 and 2290 cm^{-1}, which are from the C≡N vibration (see insert in Figure 4.11b).

As already mentioned the band at 2290 cm^{-1} originates from the C≡N vibration of the cyanopyridine group. Based on previous study in **Paper III**, were isothiocyanate SAMs are formed at a gold surface via the chemical bond of S–Au through the NCS group sulfur atoms, a nearby laying band at 2230 cm^{-1} was observed during the self-assembly process of the isothiocyanate group. Both equatorial and axial chair conformers are formed at low bulk concentrations, whereas at high concentrations the former conformation appeared to be dominant.[229] In this work, the S-C≡N- group was formed after self-assembly of the isothiocyanate monomer, therefore additional C≡N is observed in the FTIR spectra, more details can be found in **Paper III**.

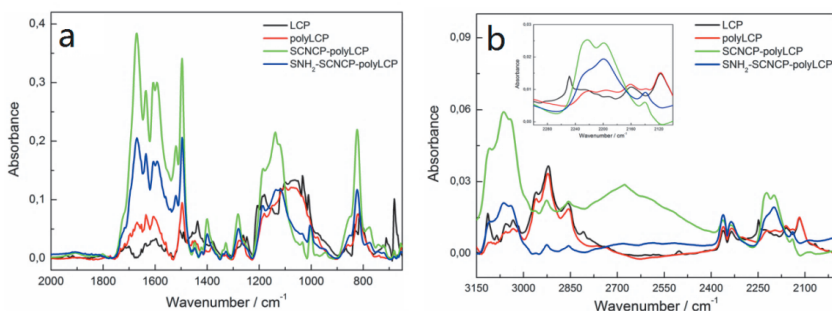**Figure 4.11.** FTIR spectra of polyviologen films grown on SNH$_2$-SCNCP and SCNCP layers from (**a**) 2200 to 650 cm^{-1} and (**b**) 3150-2000 cm^{-1} (**Paper III**)

4.5 AFM & SEM

The morphology of the synthesized viologen materials were mainly characterized by AFM and SEM. The surface of the copolyviologen is shown in Figure 4.12a. Cavities in the film can be observed which were formed when using branched monomers as precursors. As mentioned above, the AFM can also be utilized to estimate the thickness of the film. An example is shown in Figure 4.12b, where a copolyviologen film was scratched using a sharp knife after the polymerization. AFM measures the sample in X, Y and Z direction, the thickness of the copolyviologen films can be obtained by calculating the Z value between the film and the empty area. Along with the electrochemical methods, the thickness of the viologen films can in this way be roughly estimated.

The SAM film is another good example to show the ability of 3D measurement of AFM. In Figure 4.12 (c) and (d), the AFM images of the isothiocyanate monomer anchored SNH$_2$ film (SNH$_2$-SCNCP) and the polyviologen film which was electrochemically polymerized on SNH$_2$-SCNCP are shown, respectively. In Figure 4.12a, it is seen that the surface is homogenously covered by the anchor monomer. However, after the electrochemical polymerization, the film turns more rough, which

can also be seen from the SEM images in Figure 4.13c. The length of the polyviologen strings is also increasing from 25.9 nm to 91.2 nm, which indicates that a linear polymer is successfully synthesized.
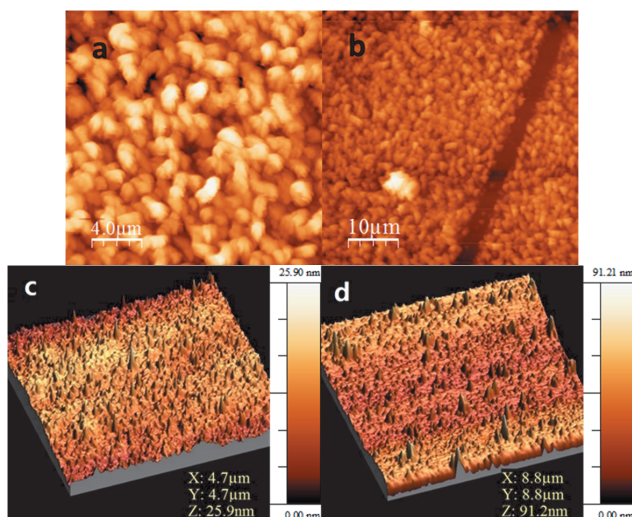

Figure 4.12. AFM images of (**a**), (**b**) copolyviologen, (**c**) SNH$_2$-SCNCP and (**d**) SNH$_2$-SCNCP-polyLCP on Au.

In the SEM images in Figure 4.13 d, it can be observed that the film consists of two layers; the brush like outwards extending strands consisting of SNH$_2$-SCNCP-polyLCP and a thin layer covering the rest of the surface. This thin layer might be a result of a reaction between the amine group (SNH$_2$) and the cyano group (SCNCP).[230] It has been shown that a reaction between these two groups can take place. [231] Additionally, as this reaction leads to a stable compound having the SCN group as outwards extending ends, that does not undergo polymerization with the cyano group at the LCP thus blocking the formation of the long polyviologen strands.

The changes in morphology of the viologen materials are not only studied by AFM but also by SEM. In Figure 4.13, the different samples of the viologen materials (polyviologens, SAM grafted polyviologen and viologen based composited material) are measured by SEM. Figure 4.12a shows the thickness of the electrochemically synthesized polyviologen films, the thickness can be estimated by detaching the film. In Figure 4.13b, the surface of the polyviologen is imaged. It can be observed that the polyviologen film is very porous, which confirms the idea that polyviologens can work as good matrix materials for molecules and proteins. Possessing unique redox property, polyviologen is an excellent candidate in applications as sensors and fuel cells.

As described above, the variations in thickness during the SAM process can easily be detected by AFM. However, by SEM analysis it is more efficient to analyze surface changes on a broader scale. As an example, Figure 4.13c shows the surface morphology of the SAM grafted polyviologen film, with which the brush shaped linear structure can easily be distinguished. Additionally, for ultra-thin materials, such like rGO having a thickness of a few nanometers SEM can be used to detect the existence of such thin materials. As shown in Figure 4.13d, the un-regular particles and the overlapping layers shows that the reduced graphene oxide has been successfully immobilized in the polyviologen film, indicating a successful synthesis of the composite materials. More details about the surface morphology of the PV-rGO composite film can be found in **Paper IV**.

Figure 4.13. SEM images of (**a**) PolyFCP, (**b**) PolyFCP, (**c**) SNH$_2$-SCNCP-polyLCP on Au and (**d**) composited film based on polyviologen and reduced graphene oxide

4.6 Conductivity measurements

The conductivity is an important parameter which limits the application of viologen materials. However, it is assumed that the conductivity of viologen materials will be different at each redox state. As described above, the first redox process, involving the reduction of the dication form to radical cation form, induces a switch of the two pyridine rings into a planar structure. A pi-conjugated molecule orbital may be formed between the two pyridine rings, through which the conductivity of the polyviologen

can be increased. In order to characterize the conductivity change during the first redox process, the *in situ* conductivity measurement, computer modeling and EIS measurement can be combined together to characterize the conductivity of the viologen materials.[42, 131, 232, 233]

The *in situ* conductivity measurement were carried out using a in house designed bi-electrode system, which is based on the theories of conformal mapping and elliptic integrals.[234] Two Pt electrodes are placed parallel with a spacer (3 µm and 5 µm), and the current between these two electrodes is measured with a multimeter. When the electrochemical polymerization is carried out covering the electrodes, the films can grow on the two Pt electrodes separately. When the films are thick enough to overlap the gap, the signal from the multimeter can be detected. Based on previous results,[234] the conductance is linearly related to the logarithm of the thickness of the film. Additionally, it has been proven that the conductivity of the viologen is switchable and a maximum value can be obtained in the radical cation form.[233] However, comparing to conducting polymers, the conductivity of polyviologen is rather low, making it difficult to measure the conductance change during the redox process. Additionally, as shown above in the SEM and AFM part, the polyviologen has a porous structure, which means that the connection between the electrode gaps is very weak and brittle. All of these factors lead to the difficulty to reliably measure and calculate the conductivity of the polyviologen materials. In order to confirm the conductance change during the redox process, impedance spectroscopy was also measured for the polyviologens.

Another attempt to characterize the effect of the redox activity on the conductivity of the viologen materials is through the EIS measurement, which is explained in **Paper IV**. This technique is very sensitive for charge transfer processes taking place between the modified electrode and the solution face. In the experiment, the Nyquist plots from the EIS measurement of a polyviologen (TPV) and of a composite film (TPV/rGO) were measured. Similar as the results shown in the UV-vis part, the performances of the polyviologens and composite films are changing according to the potentials which were applied on the films. The signal is decreasing rapidly at the beginning until -0.4 V, at which the signal is slightly increasing. After this the signal is continuously decreasing until -0.8 V, after which an increase in the signal takes place until -1.0 V is reached. The composite film shows a similar two-step process performance. However, it should be mentioned that the resistance is lower and the slopes of the curves are generally higher. This can be explained by introduction of rGO, which increase the conductivity of the composite film.

However, in these measurements, the semicircle at high frequencies cannot be obtained due to the porous structure strongly influencing the electron transfer. This results in that the spectrum cannot be easily fitted, so the result is not further discussed in this work.

4.7 Other methods

In this work, several other techniques were applied for material characterization from which the contact angle measurement and Raman spectroscopy will be shortly discussed.

Contact angle

The contact angle measurement is widely utilized in the characterization of surface morphology, especially when studying SAMs (**Paper III**). As described in the previous part, the SAM process was applied to modify the electrode surface for the electrochemical polymerization. With the help of contact angle measurements, the SAM process can be easily followed and detected. Figure 4.14a and b show the contact angels of monolayers of SCNCP self-assembled on gold surfaces for 1h and 5h, respectively. The tension of the water droplets have changed and the degree of the contact angle has notably decreased with deposition time. In Figure 4.14c, the changes in the contact angle with time, during the SAM process (SCNCP on gold surface) is plotted. By increasing the immersing time, the concentration of monomer immobilized on the gold surface is increasing. By the contact angle measurement, the SAM process can be conveniently controlled and the most suitable time for immersion can be determined.
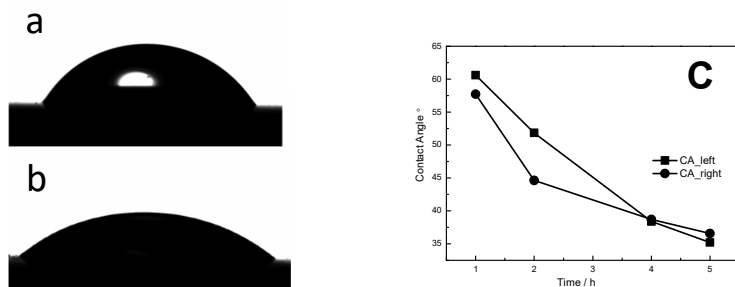

Figure 4.14. Contact angle measurements of the self-assembled SCNCP at 1h (**a**) and 5h (**b**), and the change in contact angle during the SAM process (**c**).

Raman spectroscopy

The Raman spectroscopy technique is important for determining carbon backbone in semiconducting and redox polymers. For carbon materials there are two important features in the Raman spectra: G band and D band. The G band is due to the sp^2 carbon system, which is from the C-C stretching. The D band is due to the disordered sp^2-hybridized carbon system, which is from the disordered structure of the carbon materials. With the measurement of the G band and the D band, the structure change of the carbon materials can be easily detected by Raman spectroscopy. In this work, Raman spectroscopy was introduced to distinguish the rGO in the composite film (**Paper IV**). In Figure 4.15, the Raman spectra of polyviologen and the polyviologen/rGO based composite films are shown. The G band can be observed at arround1650 cm^{-1} and the D band at 1300 cm^{-1}, for the polyviologen. However, for the composite film, the G band and D band can be observed at 1600 cm^{-1} and 1290 cm^{-1}, respectively. The reasons for the shifts observed in the spectra can be explained by the immobilization of rGO, which confirms the successful introduction of rGO in the composite film.
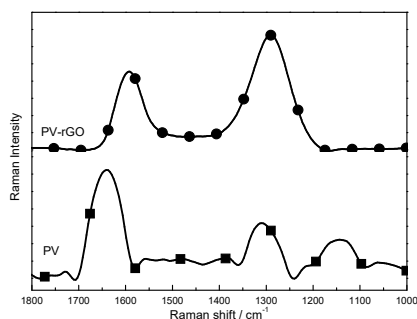

Figure 4.15. Raman spectroscopy of the polyviologens (PV) and composite film (PV-rGO).

5.   Conclusions and future research plans

In this work, a series of viologen materials were successfully synthesized and thoroughly characterized mainly by electrochemical and spectroscopic methods. The studied viologen materials showed good and reproducible redox properties. The viologen materials, especially the polyviologen films, have shown huge potential when to be applied in varies electronics as the functional materials due to their stable redox properties and unique porous structures. The PV-rGO based composite film has shown good electrochemical properties which can be utilized in varies electronics. Based on the publications, the conclusions are:

1.   The good stability and the reversible redox process of the polyviologens have been proved in **Paper I** and **II** that enable them to work as mediators in sensors and in fuel cells.

2.   The cavity size of the films can be adjusted by using differently substituted cyanopyridine monomers in the electrochemical synthesis, or by building up copolymer structures using different types of monomers.

     The electrochemical characterization using electrolytes with various anion sizes indicates changes in the cavity dimensions of the films. Such polyviologen films have strong potential to be applied as immobilization materials for large particles or biological molecules.

3.   The polyviologen film, which was prepared based on the SAM modified electrode concept showed a unique structure, which indicate that the structure of the polyviologen can be controlled and tuned towards special structures. This enables polyviologens to be utilized under special conditions with need of outwards extending structures.

4.   The composite film based on the polyviologen and rGO showed a stable and enhanced redox property, which shows possibility of this viologen material to be applied in energy storage devices.

The electrochemical synthesis based on CP-monomers has revealed a new efficient way to prepare polyviologen materials with tuned properties. In **Paper III** it was proved the PV of well-ordered structure can be formed even on other functional materials having an amine functionalization. Based on the same concept, the polyviologen materials can be covalently bond to biological materials forming stable bio-composites.

In **Paper I** and **II**, the porous structures obtained from the branched PVs resulted in materials with high surface area. In **Paper II**, it was shown that the different electrolytes not only had an effect on the structure of PVs but also on the open circuit potential of the materials. This opens up a possibility of maintaining a specific potential of PV by tuning of the electrolyte. Additionally, it has been shown in **Paper IV** that the charge capability of PV-rGO can be enhanced by using rGO. The above mentioned advantages are all profitable for materials used in supercapacitors. The following research will be focused on this application.

6. Reference

1. P. M. S. Monk, The viologens: physicochemical properties, synthesis, and applications of the salts of 4, 4'-bipyridine, John Wiley & sons Ltd, West Sussex, England, 1998.

2. C. L. Bird and A. T. Kuhn, Chemical Society reviews, 1981, **10**, 49-82.

3. P. Monk, R. Mortimer and D. Rosseinsky, Electrochromism and electrochromic devices, Cambridge University Press, 2007.

4. P. Monk, D. R. Rosseinsky and R. J. Mortimer, Electrochromic Materials and Devices, 2015, 57-90.

5. S. W. T. III, G. D. Joly and T. M. Swager, Chem. Rev, 2007, **107**, 1339-1386.

6. S. M. Kim, J. H. Jang, K. K. Kim, H. K. Park, J. J. Bae, W. J. Yu, I. H. Lee, G. Kim, D. D. Loc, U. J. Kim, E.-H. Lee, H.-J. Shin, J.-Y. Cho and Y. H. Lee, journal of American Society, 2009, **131**, 327-331.

7. V.-A. Constantin, L. Cao, S. Sadaf and L. Walder, physica status solidi (b), 2012, **249**, 2395-2398.

8. H. K. Jeong, K.-j. Kim, S. M. Kim and Y. H. Lee, Chemical Physics Letters, 2010, **498**, 168-171.

9. H. Li, Z. Zhu, A. C. Fahrenbach, B. M. Savoie, C. Ke, J. C. Barnes, J. Lei, Y. L. Zhao, L. M. Lilley, T. J. Marks, M. A. Ratner and J. F. Stoddart, Journal of the American Chemical Society, 2013, **135**, 456-467.

10. A. E. Kaifer, Acc Chem Res, 2014, **47**, 2160-2167.

11. M. Freitag, L. Gundlach, P. Piotrowiak and E. Galoppini, Journal of the American Chemical Society, 2012, **134**, 3358-3366.

12. A. C. Fahrenbach, S. Sampath, D. J. Late, J. C. Barnes, S. L. Kleinman, N. Valley, K. J. Hartlieb, Z. Liu, V. P. Dravid, G. C. Schatz, R. P. V. Duyne and J. F. Stoddart, ACS NANO, 2012, **6**, 9964-9971.

13. H. Li, D. X. Chen, Y. L. Sun, Y. B. Zheng, L. L. Tan, P. S. Weiss and Y. W. Yang, Journal of the American Chemical Society, 2013, **135**, 1570-1576.

14. M. Elstner, K. Weisshart, K. Mullen and A. Schiller, Journal of the American Chemical Society, 2012, **134**, 8098-8100.

15. E. Hwang, S. Seo, S. Bak, H. Lee, M. Min and H. Lee, Adv Mater, 2014, **26**, 5129-5136.

16. H. C. Moon, C. H. Kim, T. P. Lodge and C. D. Frisbie, ACS applied materials & interfaces, 2016, **8**, 6252-6260.

17. D. Corr, U. Bach, D. Fay, M. Kinsella, C. McAtamney, F. O'Reilly, S. N. Rao and N. Stobie, Solid State Ionics, 2003, **165**, 315-321.

18. T. Higashi and T. Sagara, Langmuir : the ACS journal of surfaces and colloids, 2013, **29**, 11516-11524.

19. J. Palenzuela, A. Vinuales, I. Odriozola, G. Cabanero, H. J. Grande and V. Ruiz, ACS applied materials & interfaces, 2014, **6**, 14562-14567.

20. R. Vergaz, D. Barrios, J.-M. Sánchez-Pena, C. Pozo-Gonzalo and M. Salsamendi, Solar Energy Materials and Solar Cells, 2009, **93**, 2125-2132.

21. R. J. Mortimer, A. L. Dyer and J. R. Reynolds, Displays, 2006, **27**, 2-18.

22. M. Möller, S. Asaftei, D. Corr, M. Ryan and L. Walder, Adv Mater, 2004, **16**, 1558-1562.

23. J.-M. Zen and C.-W. Lo, Anal. Chem., 1996, **68**, 2635-2640.

24. D. J. Qian, C. Nakamura, S. O. Wenk, H. Ishikawa, N. Zorin and J. Miyake, Biosensors & bioelectronics, 2002, **17**, 789-796.

25. Q. Wu, G. D. Storrier, F. Pariente, Y. Wang, J. P. Shapleigh and H. D. Abruna, Analytical Chemistry, 1997, **69**, 4856-4863.

26. B. Strehlitz, B. Grundig, W. Schumacher, P. M. H. Kroneck, K.-D. Vorlop and H. Kotte, Anal. Chem., 1996, **68**, 807-816.

27. S. Tsujimura, M. Fujita, H. Tatsumi, K. Kano and T. Ikeda, Physical Chemistry Chemical Physics, 2001, **3**, 1331-1335.

28. X. Liu, M. Hao, M. Feng, L. Zhang, Y. Zhao, X. Du and G. Wang, Applied Energy, 2013, **106**, 176-183.

29. Y.-K. Oh, Y.-j. Lee, E.-H. Choi and M.-S. Kim, International Journal of Hydrogen Energy, 2008, **33**, 5218-5223.

30. D. R. Wheeler, J. Nichols, D. Hansen, M. Andrus, S. Choi and G. D. Watt, Journal of the Electrochemical Society, 2009, **156**, 1201-1207.

31. A. Wieckowska, A. B. Braunschweig and I. Willner, Chemical Communications, 2007, DOI: .1039/B710540A, 3918-3920.

32. U. Carragher, Doctor of Philosophy, National University of Ireland, 2013.

33. G. Liu, C. Wang, W. Zhang, L. Pan, C. Zhang, X. Yang, F. Fan, Y. Chen and R.-W. Li, Advanced Electronic Materials, 2015, DOI: 10.1002/aelm.201500298, 1500298.

34. Y. Luo, P. C. Collier, J. O. Jeppesen, K. A. Nielsen, E. Delonno, G. Ho, J. Perkins, H. R. Tseng, T. Yamamoto, J. F. Stoddart and J. R. Heath, Chemphyschem : a European journal of chemical physics and physical chemistry, 2002, **3**, 519-525.

35. C. Cheng, P. R. McGonigal, W. G. Liu, H. Li, N. A. Vermeulen, C. Ke, M. Frasconi, C. L. Stern, W. A. Goddard, 3rd and J. F. Stoddart, Journal of the American Chemical Society, 2014, **136**, 14702-14705.

36. J. C. Barnes, M. Juricek, N. L. Strutt, M. Frasconi, S. Sampath, M. A. Giesener, P. L. McGrier, C. J. Bruns, C. L. Stern, A. A. Sarjeant and J. F. Stoddart, Journal of the American Chemical Society, 2013, **135**, 183-192.

37. W. W. Porter, T. P. Vaid and A. L. Rheingold, Journal of the American Chemical Society, 2005, **127**, 16559-16566.

38. D. Cummins, G. Boschloo, M. Ryan, S. David Corr, N. Rao and D. Fitzmaurice, Journal of Physical Chemistry B, 2000, **104**, 11449-11459.

39. N. Sano, Doctoral Doctoral Thesis, Waseda University, 2013.

40. B. Xu, L. Xu, G. Gao, Y. Yang, W. Guo, S. Liu and Z. Sun, Electrochimica Acta, 2009, **54**, 2246-2252.

41. D. R. Rosseinsky, P. M. S. Monk and R. A. Hann, Electrochimica Acta, 1990, **35**, 1113-1123.

42. V.-A. Constantin, D. Bongard and L. Walder, European Journal of Organic Chemistry, 2012, **2012**, 913-921.

43. M. Nanasawa, Y. Matsukawa, J. J. Jin and Y. Haramoto, Journal of Photochemistry and Photobiology A: Chemistry, 1997, **109**, 35-38.

44. J. P. Hallett and T. Welton, Chemical reviews, 2011, **111**, 3508-3576.

45. J. Park, S. Ko and J.-Y. Park, Bulletin of the Korean Chemical Society, 1992, **13**, 259-265.

46. H. Kamogawa and S. Sato, B Chem Soc Jpn, 1991, **64**, 321-323.

47. G. A. Snook, P. Kao and A. S. Best, Journal of Power Sources, 2011, **196**, 1-12.

48. R. J. Mortimer, Chem. Soc. Rev., 1997, **26**, 147-156.

49. R. J. Mortimer, Electrochimica Acta, 1999, **44**, 2971-2981.

50. V. K. Thakur, G. Ding, J. Ma, P. S. Lee and X. Lu, Advanced Materials, 2012, **24**, 4071-4096.

51. P. Monk, R. Mortimer and D. Rosseinsky, Electrochromism and electrochromic devices, Cambridge University Press, 2007.

52. M. E. Lyons, in Electroactive polymer electrochemistry, Springer, 1994, pp. 237-374.

53. R. N. Vyas and B. Wang, International journal of molecular sciences, 2010, **11**, 1956-1972.

54. P. M. S. Monk, R. J. Mortimer and D. R. Rosseinsky, in Electrochromism, Wiley-VCH Verlag GmbH, 2007, DOI: 10.1002/9783527615377.ch8, pp. 124-142.

55. A. E. Kaifer and A. J. Bard, J. Phys. Chem., 1985, **89**, 4876-4880.

56. Y. Okahata and G.-i. En-na, Journal of physical Chemistry, 1988, **92**, 4546-4551.

57. V. Sindelar, K. Moon and A. E. Kaifer, Organic Letters, 2004, **6**, 2665-2668.

58. H. Tokue, K. Oyaizu, T. Sukegawa and H. Nishide, ACS applied materials & interfaces, 2014, **6**, 4043-4049.

59. M. Freitag and E. Galoppini, Langmuir : the ACS journal of surfaces and colloids, 2010, **26**, 8262-8269.

60. R. H. REUSS and L. J. WINTERS, J. Org. Chem, 1973, **38**, 3993-3995.

61. R. H. Reuss, N. G. Smith and L. J. Winters, J. Org. Chem, 1974, **39**, 2027-2031.

62. T. Masuda, K. Shimazu and K. Uosaki, J. Phys. Chem. C, 2008, **112**, 10923-10930.

63. T. Masuda, M. Irie and K. Uosaki, Thin Solid Films, 2009, **518**, 591-595.

64. T. Masuda, H. Fukumitsu, S. Takakusagi, W. J. Chun, T. Kondo, K. Asakura and K. Uosaki, Adv Mater, 2012, **24**, 268-272.

65. Y. Sun, T. Masuda and K. Uosaki, Chemistry Letters, 2012, **41**, 328-330.

66. B. Zhao, K. G. Neoh and E. T. Kang, Journal of Applied Polymer Science, 2002, **86**, 2099-2107.

67. L. Cen, K. G. Neoh and E. T. Kang, Biosensors and Bioelectronics, 2003, **18**, 363-374.

68. I. Yamaguchi, H. Higashi, S. Shigesue, S. Shingai and M. Sato, Tetrahedron Letters, 2007, **48**, 7778-7781.

69. I. Yamaguchi, H. Higashi and M. Sato, Reactive and Functional Polymers, 2009, **69**, 864-869.

70. D. Bongarda, M. Möllera, S. N. Rao, D. Corrb and LorenzWalder, HELVETICA CHIMICA ACTA, 2005, **88**, 3200-3209.

71. V.-A. Constantin, Doctor, 2012.

72. A. Reisch, M. D. Moussallem and J. B. Schlenoff, Langmuir : the ACS journal of surfaces and colloids, 2011, **27**, 9418-9424.

73. L.-p. Gao, G.-j. Ding, C.-l. Li and Y.-c. Wang, Applied Surface Science, 2011, **257**, 3039-3046.

74. T. Ohsaka, H. Yamamoto and N. Oyama, J. Phys. Chem., 1987, **91**, 3775-3779.

75. C. D. Clark, J. D. Debad, E. H. Yonemoto, T. E. Mallouk and A. J. Bard, J. AM. CHEM. SOC., 1997, **119**, 10525-10531.

76. H.-Y. Li, Y.-L. Wei, X.-Y. Dong, S.-Q. Zang and T. C. Mak, Chemistry of Materials, 2015, **27**, 1327-1331.

77. H. C. Ko, S.-a. Park, W.-k. Paik and H. Lee, Synthetic Metals, 2002, **132**, 15-20.

78. N. S. Sariciftci, A. C. Kolbert, M. Mehring, K. U. Gaudl, P. Btiuerle, H. Neugebauer and A. Neckel, Chemical Physics Letters, 1991, **182**, 326-330.

79. N. S. Sariciftci, M. Mehring, K. U. Gaudl, P. Bäuerle, H. Neugebauer and A. Neckel, Journal of Chemical Physics, 1992, **96**, 7164-7170.

80. B. Gadgil, P. Damlin, T. Ääritalo, J. Kankare and C. Kvarnström, Electrochimica Acta, 2013, **97**, 378-385.

81. S. Cosnier, S. Da Silva, D. Shan and K. Gorgy, Bioelectrochemistry, 2008, **74**, 47-51.

82. C. Gondran, M. Orio, D. Rigal, B. Galland, L. Bouffier, T. Gulon and S. Cosnier, Electrochemistry Communications, 2010, **12**, 311-314.

83. S. Da Silva, D. Shan and S. Cosnier, Sensors and Actuators B: Chemical, 2004, **103**, 397-402.

84. S. Cosnier, M. Dawod, K. Gorgy and S. Da Silva, Microchimica Acta, 2003, **143**, 139-145.

85. S. Cosnier, Biosensors and Bioelectronics, 1999, **14**, 443-456.

86. S. Cosnier, C. Gondran and A. Senillou, Synthetic metals, 1999, **102**, 1366-1369.

87. Z. Shi, K. G. Neoh and E. T. Kang, Biomaterials, 2005, **26**, 501-508.

88. X. Liu, K. G. Neoh, L. Zhao and E. T. Kang, Langmuir : the ACS journal of surfaces and colloids, 2002, **18**, 2914-2921.

89. X. Liu, K. G. Neoh and E. T. Kang, Langmuir : the ACS journal of surfaces and colloids, 2002, **18**, 9041-9047.

90. B. Zhao, K. G. Neoh, F. T. Liu, E. T. Kang and K. L. Tah, Synthetic Metals, 2001, **123**, 263-266.

91. H. Shirakawa, E. J. Louis, A. G. MacDiarmid, C. K. Chiang and A. J. Heeger, Journal of the Chemical Society, Chemical Communications, 1977, 578-580.

92. J. Janata and M. Josowicz, Nature materials, 2003, **2**, 19-24.

93. S. Gu¨nes, H. Neugebauer and N. S. Sariciftci, Chem. Rev, 2007, **107**, 1324-1338.

94. B. S. Ong, Y. Wu, P. Liu and S. Gardner, Journal of the American Chemical Society, 2004, **126**, 3378-3379.

95. J. Chen, Y. Liu, A. I. Minett, C. Lynam, J. Wang and G. G. Wallace, Chemistry of Materials, 2007, **19**, 3595-3597.

96. C. Tan and D. Blackwood, Corrosion Science, 2003, **45**, 545-557.

97. M. A. Vorotyntsev, V. A. Zinovyeva and D. V. Konev, in Electropolymerization, Wiley-VCH Verlag GmbH & Co. KGaA, 2010, DOI: 10.1002/9783527630592.ch2, pp. 27-50.

98. H. Murakami, A. Kawabuchi, R. Matsumoto, T. Ido and N. Nakashima, J. AM. CHEM. SOC., 2005, **127**, 15891-15899.

99. J. r. Heinze, B. A. Frontana-Uribe and S. Ludwigs, Chemical reviews, 2010, **110**, 4724-4771.

100. S. Cosnier and A. Karyakin, Electropolymerization: concepts, materials and applications, John Wiley & Sons, 2011.

101. G. Bidan, in Electropolymerization, Wiley-VCH Verlag GmbH & Co. KGaA, 2010, DOI: 10.1002/9783527630592.ch1, pp. 1-26.

102. E. M. Kosower and J. L. Cotter, Journal of the American Chemical Society, 1964, **86**, 5524-5527.

103. K. Kamata, T. Suzuki, T. Kawai and T. Iyoda, Journal of Electroanalytical Chemistry, 1999, **473**, 145–155.

104. Y.-C. Hsu and K.-C. Ho, Journal of New Materials for Electrochemical System, 2005, **8**, 49-57.

105. N. Sano, W. Tomita, S. Hara, C. M. Min, J. S. Lee, K. Oyaizu and H. Nishide, ACS applied materials & interfaces, 2013, **5**, 1355-1361.

106. K. Kamata, T. Kawai and T. Iyoda, Langmuir : the ACS journal of surfaces and colloids, 2001, **17**, 155-163.

107. R. G. Nuzzo and D. L. Allara, Journal of the American Chemical Society, 1983, **105**, 4481-4483.

108. A. Ulman, Chemical reviews, 1996, **96**, 1533-1554.

109. J. Love, L. Estroff, J. Kriebel, R. Nuzzo and G. Whitesides, Chemical reviews, 2005, **105**, 1103-1169.

110. B. B. Narakathu, M. S. Devadas, A. S. G. Reddy, A. Eshkeiti, A. Moorthi, I. R. Fernando, B. P. Miller, G. Ramakrishna, E. Sinn and M. Joyce, Sensors and Actuators B: Chemical, 2013, **176**, 768-774.

111. P. Ardalan, T. P. Brennan, H.-B.-R. Lee, J. R. Bakke, I.-K. Ding, M. D. McGehee and S. F. Bent, ACS NANO, 2011, **5**, 1495–1504.

112. C. Wendeln, S. Rinnen, C. Schulz, H. F. Arlinghaus and B. J. Ravoo, Langmuir : the ACS journal of surfaces and colloids, 2010, **26**, 15966-15971.

113. A. K. M. Kafi, D.-Y. Lee, S.-H. Park and Y.-S. Kwon, Microchemical Journal, 2007, **85**, 308-313.

114. B. Liu, A. Blaszczyk, M. Mayor and ThomasWandlowski, ACS NANO, 2011, **5**, 5662-5672.

115. Z. Mai, X. Zhao, Z. Dai and X. Zou, Talanta, 2010, **81**, 167-175.

116. W. S. Jeon, A. Y. Ziganshina, J. W. Lee, Y. H. Ko, J.-K. Kang, C. Lee and K. Kim, Angewandte Chemie, 2003, **115**, 4231-4234.

117. J. Li, J. Yan, Q. Deng, G. Cheng and S. Dong, Electrochimica Acta, 1996, **42**, 961-967.

118. N. Nakamura, H.-X. Huang, D.-J. Qian and J. Miyake, Langmuir : the ACS journal of surfaces and colloids, 2002, **18**, 5804-5809.

119. K.-H. Hyung, D.-Y. Kim and S.-H. Han, New Journal of Chemistry, 2005, **29**, 1022-1026.

120. K. A. B. Lee, Langmuir : the ACS journal of surfaces and colloids, 1990, **6**.

121. M. H. Chakrabarti, R. A. W. Dryfe and E. P. L. Roberts, Electrochimica Acta, 2007, **52**, 2189-2195.

122. J. Noack, N. Roznyatovskaya, T. Herr and P. Fischer, Angew Chem Int Ed, 2015, **54**, 9776-9809.

123. C. Ponce de León, A. Frías-Ferrer, J. González-García, D. A. Szánto and F. C. Walsh, Journal of Power Sources, 2006, **160**, 716-732.

124. T. Welton, Chemical reviews, 1999, **99**, 2071-2084.

125. M. Armand, F. Endres, D. R. MacFarlane, H. Ohno and B. Scrosati, Nature materials, 2009, **8**, 621-629.

126. M. Egashira, S. Okada, J.-i. Yamaki, D. A. Dri, F. Bonadies and B. Scrosati, Journal of power sources, 2004, **138**, 240-244.

127. L. Cecchetto, M. Salomon, B. Scrosati and F. Croce, Journal of Power Sources, 2012, **213**, 233-238.

128. Y. Pang, X. Li, H. Ding, G. Shi and L. Jin, Electrochimica acta, 2007, **52**, 6172-6177.

129. L. Ma, Y. Li, X. Yu, Q. Yang and C.-H. Noh, Solar Energy Materials and Solar Cells, 2009, **93**, 564-570.

130. S. T. Handy, Chemistry–A European Journal, 2003, **9**, 2938-2944.

131. R. Sydam, M. Deepa and A. G. Joshi, Organic Electronics, 2013, **14**, 1027-1036.

132. H. Tahara, H. Yonemura, S. Harada, A. Nakashima and S. Yamada, Chemical Physics Letters, 2012, **524**, 42-48.

133. S. R. Shin, C. K. Lee, S. I. Kim, I. So, G. M. Spinks, G. G. Wallace and S. J. Kim, Langmuir : the ACS journal of surfaces and colloids, 2008, **24**, 3562-3565.

134. A. Kavanagh, K. J. Fraser, R. Byrne and D. Diamond, ACS applied materials & interfaces, 2013, **5**, 55-62.

135. H. Q. N. Gunaratne, P. Nockemann, S. Olejarz, S. M. Reid, K. R. Seddon and G. Srinivasan, Australian Journal of Chemistry, 2013, DOI: 10.1071/ch13054.

136. K. S. Novoselov, A. K. Geim, S. Morozov, D. Jiang, Y. Zhang, S. a. Dubonos, I. Grigorieva and A. Firsov, science, 2004, **306**, 666-669.

137. K. S. Novoselov, V. I. Fal'ko, L. Colombo, P. R. Gellert, M. G. Schwab and K. Kim, Nature, 2012, **490**, 192-200.

138. V. Georgakilas, M. Otyepka, A. B. Bourlinos, V. Chandra, N. Kim, K. C. Kemp, P. Hobza, R. Zboril and K. S. Kim, Chemical reviews, 2012, **112**, 6156-6214.

139. A. K. GEIM and K. S. NOVOSELOV, Nature materials, 2007, **6**, 183-191.

140. K. P. Loh, Q. Bao, G. Eda and M. Chhowalla, Nature chemistry, 2010, **2**, 1015-1024.

141. P. Han, H. Wang, Z. Liu, X. Chen, W. Ma, J. Yao, Y. Zhu and G. Cui, Carbon, 2011, **49**, 693-700.

142. Y. Shao, J. Wang, H. Wu, J. Liu, I. A. Aksay and Y. Lin, Electroanalysis, 2010, **22**, 1027-1036.

143. D. A. C. Brownson, D. K. Kampouris and C. E. Banks, Journal of Power Sources, 2011, **196**, 4873-4885.

144. D. Chen, H. Feng and J. Li, Chemical reviews, 2012, **112**, 6027-6053.

145. M. F. El-Kady, V. Strong, S. Dubin and R. B. Kaner, Science, 2012, **335**, 1326-1330.

146. X. Huang, Z. Zeng, Z. Fan, J. Liu and H. Zhang, Adv Mater, 2012, **24**, 5979-6004.

147. T. Kuilla, S. Bhadra, D. Yao, N. H. Kim, S. Bose and J. H. Lee, Process in Polymer Science, 2010, **35**, 1350-1375.

148. X. Huang, X. Qi, F. Boey and H. Zhang, Chemical Society reviews, 2012, **41**, 666-686.

149. M. Wang, X. Duan, Y. Xu and X. Duan, ACS Nano, 2016, **10**, 7231-7247.

150. X. WAN, Y. HUANG and Y. CHEN, Acc. Chem. Res., 2011, **45**, 598-607.

151. D. R. Dreyer, S. Park, C. W. Bielawski and R. S. Ruoff, Chemical Society reviews, 2010, **39**, 228-240.

152. M. Pumera, Chemical Society reviews, 2010, **39**, 4146-4157.

153. D. WEI, B. WU, Y. GUO, G. YU and Y. LIU, Acc. Chem. Res., 2012, **46**, 106-115.

154. V. Chabot, D. Higgins, A. Yu, X. Xiao, Z. Chen and J. Zhang, Energy & Environmental Science, 2014, **7**, 1564-1596.

155. J. Kauppila, P. Kunnas, P. Damlin, A. Viinikanoja and C. Kvarnström, Electrochimica Acta, 2013, **89**, 84-89.

156. A. Viinikanoja, Z. Wang, J. Kauppila and C. Kvarnström, Physical Chemistry Chemical Physics, 2012, **14**, 14003-14009.

157. C. K. Chua and M. Pumera, Chemical Society reviews, 2014, **43**, 291-312.

158. I. Giner, G. Pera, C. Lafuente, M. C. Lopez and P. Cea, Journal of colloid and interface science, 2007, **315**, 588-596.

159. S. A. John, F. Kitamura, K. Tokuda and T. Ohsaka, Journal of Electroanalytical Chemistry, 2000, **492**, 137-144.

160. D. T. Pham, S. L. Tsay, K. Gentz, C. Zoerlein, S. Kossmann, J. S. Tsay, B. Kirchner, K. Wandelt and P. Broekmann, Journal of Physical Chemistry C, 2007, **111**, 16428-16436.

161. P. D. Thanh, Doctoral, Rheinischen Friedrich‐Wilhelms‐Universität Bonn, 2011.

162. B. Han, Z. Li, T. Wandlowski, A. Błaszczyk and M. Mayor, J. Phys. Chem. C, 2007, **111**, 13855-13863.

163. A. J. Bard and L. R. Faulkner, Electrochemical methods : fundamentals and applications, John Wiley & Sons, Inc., USA, 2001.

164. M. Nanasawa, Organic Photochromic and Thermochromic Compounds, 2002.

165. P. M. S. Monk, R. J. Mortimer and D. R. Rosseinsky, in Electrochromism, Wiley-VCH Verlag GmbH, 2007, DOI: 10.1002/9783527615377.index, pp. 203-216.

166. M. Passon, A. Ruff, P. Schuler, B. Speiser and W. Leis, Journal of Solid State Electrochemistry, 2014, **19**, 85-101.

167. N. Chaniotakis and N. Sofikiti, Anal Chim Acta, 2008, **615**, 1-9.

168. J. Bruinink, C. G. A. Kregting and J. J. Ponje, J. Electroanal. Soc., 1977, **124**, 1854-1858.

169. S. A. John, F. Kitamura, K. Tokuda and T. Ohsaka, Langmuir : the ACS journal of surfaces and colloids, 2000, **16**, 876-880.

170. H. Takashima, M. Tanaka, Y. Hasegawa and K. Tsukahara, Journal of biological inorganic chemistry : JBIC : a publication of the Society of Biological Inorganic Chemistry, 2003, **8**, 499-506.

171. D. Taffa, M. Kathiresan and L. Walder, Langmuir : the ACS journal of surfaces and colloids, 2009, **25**, 5371-5379.

172. H.-C. Chang, T.-J. Cheng and R.-J. Chen, Electroanalysis, 1998, **10**, 1275-1280.

173. A. Trabolsi, N. Khashab, A. C. Fahrenbach, D. C. Friedman, M. T. Colvin, K. K. Coti, D. Benitez, E. Tkatchouk, J. C. Olsen, M. E. Belowich, R. Carmielli, H. A. Khatib, W. A. Goddard, 3rd, M. R. Wasielewski and J. F. Stoddart, Nature chemistry, 2010, **2**, 42-49.

174. A. T. Buck, J. T. Paletta, S. A. Khindurangala, C. L. Beck and A. H. Winter, Journal of the American Chemical Society, 2013, **135**, 10594-10597.

175. N. Wang, A. Kähkönen, P. Damlin, T. Ääritalo, J. Kankare and C. Kvarnström, Electrochimica Acta, 2015, **154**, 361-369.

176. G. Barin, M. Frasconi, S. M. Dyar, J. Iehl, O. Buyukcakir, A. A. Sarjeant, R. Carmieli, A. Coskun, M. R. Wasielewski and J. F. Stoddart, Journal of the American Chemical Society, 2013, **135**, 2466-2469.

177. R. Kannappan, C. Bucher, E. Saint-Aman, J.-C. Moutet, A. Milet, M. Oltean, E. Métay, S. Pellet-Rostaing, M. Lemaire and C. Chaix, New Journal of Chemistry, 2010, **34**, 1373.

178. T. Sagara, H. Maeda, Y. Yuan and N. Nakashima, Langmuir : the ACS journal of surfaces and colloids, 1999, **15**, 3823-3830.

179. T. Sagara, H. Tsuruta and N. Nakashima, Journal of Electroanalytical Chemistry, 2001, **500**, 255-263.

180. T. Sata, Y. Matsuo, T. Yamaguchi and K. Matsusaki, Journal of the Chemical Society, Faraday Transactions, 1997, **93**, 2553-2560.

181. S. A. John, F. Kitamura, N. Nanbu, K. Tokuda and T. Ohsaka, Langmuir : the ACS journal of surfaces and colloids, 1999, **15**, 3816-3822.

182. F. M. Raymo, R. J. Alvarado and E. J. Pacsial, Journal of Supramolecular Chemistry, 2002, **2**, 63-77.

183. A. Yasuda and J. e. Seto, J. Electroanal. Chem., 1990, **283**, 197-204.

184. J. L. Snover, H. Byrd, E. P. Suponeva, E. Vicenzi and M. E. Thompson, Chemistry of Materials, 1996, **8**, 1490-1499.

185. S. A. John and T. Ohsaka, Journal of Electroanalytical Chemistry, 1999, **477**, 52-61.

186. F. Terzi, C. Zanardi, B. Zanfrognini, L. Pigani, R. Seeber, J. Lukkari, T. Ääritalo and J. Kankare, J. Phys. Chem. C, 2009, **113**, 4868-4876.

187. N. Vlachopoulos, J. Nissfolk, M. Möller, A. Briançon, D. Corr, C. Grave, N. Leyland, R. Mesmer, F. Pichot, M. Ryan, G. Boschloo and A. Hagfeldt, Electrochimica Acta, 2008, **53**, 4065-4071.

188. T. Komura, T. Yamaguchi, K. Furuta and K. Sirono, Journal of Electroanalytical Chemistry, 2002, **534**, 123-130.

189. A. Merz and S. Reitmeier, Advanced Materials, 1989, **28**, 807-808.

190. D. R. Rosseinsky and R. J. Mortimer, Advanced Materials, 2001, **13**, 783-793.

191. J. Barratt and K. Dowd, Journal, 2006.

192. Y. Rong, S. Kim, F. Su, D. Myers and M. Taya, Electrochimica Acta, 2011, **56**, 6230-6236.

193. S. Y. Choi, M. Mamak, N. Coombs, N. Chopra and G. A. Ozin, Nano letters, 2004, **4**, 1231-1235.

194. J. García-Cañadas, Electrochemistry Communications, 2003, **5**, 199-202.

195. E. Smela, Advanced Materials, 1999, **11**, 1343-1345.

196. S. Xiong, S. L. Phua, B. S. Dunn, J. Ma and X. Lu, Chemistry of Materials, 2009, **22**, 255-260.

197. S. Alkan, C. A. Cutler and J. R. Reynolds, Advanced Functional Materials, 2003, **13**, 331-336.

198. J. P. Hallett and T. Welton, Chemical reviews, 2011, **111**, 3508-3576.

199. M. M. Musiani, Electrochimica Acta, 1990, **35**, 1665-1670.

200. R. J. Mortimer and J. R. Reynolds, Displays, 2008, **29**, 424-431.

201. P. M. S. Monk and N. M. Hodgkinson, Journal of Electroanalytical Chemistry, 1999, **462**, 43-54.

202. D. M. DeLongchamp, M. Kastantin and P. T. Hammond, Chemistry of Materials, 2003, **15**, 1575-1586.

203. P. M. S. Monk, R. J. Mortimer and D. R. Rosseinsky, in Electrochromism, Wiley-VCH Verlag GmbH, 2007, DOI: 10.1002/9783527615377.ch7, pp. 120-123.

204. B. H. Stuart, in Infrared Spectroscopy: Fundamentals and Applications, John Wiley & Sons, Ltd, 2005, DOI: 10.1002/0470011149.ch1, pp. 1-13.

205. R. K. Nagarale, B. Bhattacharya, N. A. Jadhav and P. K. Singh, Macromolecular Chemistry and Physics, 2011, **212**, 1751-1757.

206. L.-p. Gao, G.-j. Ding, Y.-c. Wang and Y.-l. Yang, Applied Surface Science, 2011, **258**, 1184-1191.

207. M. I. Zakirov, G. A. Shandryuk, G. N. Bondarenko, E. L. Nodova, D. V. Kryl'skii and R. V. Talroze, Polymer Science Series B, 2012, **54**, 50-60.

208. T.-H. Kuo, C.-Y. Hsu, K.-M. Lee and K.-C. Ho, Solar Energy Materials and Solar Cells, 2009, **93**, 1755-1760.

209. R. Cinnsealach, G. Boschloo, S. Nagaraja Rao and D. Fitzmaurice, Solar Energy Materials & Solar Cells, 1999, **57**, 107—125.

210. X. W. Sun and J. X. Wang, Nano letters, 2008, **8**, 1884-1889.

211. J. Wang, Analytical Electrochemistry, John Wiley & Sons, Inc., Hoboken, New Jersey, USA, Third Edition edn., 2006.

212. L. Rabinovich and O. Lev, Electroanalysis, 2001, **13**, 265-275.

213. S. Sampath and O. Lev, Journal of Electroanalytical Chemistry, 1998, **446**, 57-65.

214. N. F. Ferreyra, L. Coche-Gue´rente, P. Labbe, E. J. Calvo and V. M. Solı´s, Langmuir : the ACS journal of surfaces and colloids, 2003, **19**, 3864-3874.

215. M. D. Leonida, A. J. Fry, S. B. Sobolov and K. Voivodov, Bioorganic & medicinal chemistry letters, 1996, **6**, 1663-1666.

216. B. H. Stuart, in Infrared Spectroscopy: Fundamentals and Applications, John Wiley & Sons, Ltd, 2005, DOI: 10.1002/0470011149.ch4, pp. 71-93.

217. C. Yang, G. He, R. Wang and Y. Li, Thin Solid Films, 2000, **363**, 218-220.

218. M. A. Saab, R. Abdel-Malak, J. F. Wishart and T. H. Ghaddar, Langmuir : the ACS journal of surfaces and colloids, 2007, **23**, 10807-10815.

219. J. Chang, S. Lee, T. Ganesh, R. S. Mane, S. Min, W. Lee and S.-H. Han, Journal of Electroanalytical Chemistry, 2008, **624**, 167-173.

220. S. E. Chun, B. Evanko, X. Wang, D. Vonlanthen, X. Ji, G. D. Stucky and S. W. Boettcher, Nature communications, 2015, **6**, 7818.

221. T. Janoschka, N. Martin, U. Martin, C. Friebe, S. Morgenstern, H. Hiller, M. D. Hager and U. S. Schubert, Nature, 2015, **527**, 78-81.

222. T. Janoschka, S. Morgenstern, H. Hiller, C. Friebe, K. Wolkersdörfer, B. Häupler, M. D. Hager and U. S. Schubert, Polymer Chemistry, 2015, **6**, 7801-7811.

223. G. Fioravanti, N. Haraszkiewicz, E. R. Kay, S. M. Mendoza, C. Bruno, M. Marcaccio, P. G. Wiering, F. Paolucci, P. Rudolf, A. M. Brouwer and D. A. Leigh, J. AM. CHEM. SOC., 2008, **130**, 2593-2601.

224. W. Ong, J. Grindstaff, D. Sobransingh, R. Toba, J. M. a. Quintela, C. Peinador and A. E. Kaifer, J. AM. CHEM. SOC., 2005, **127**, 3353-3361.

225. I. Maeng, S. Lim, S. J. Chae, Y. H. Lee, H. Choi and J. H. Son, Nano letters, 2012, **12**, 551-555.

226. B. H. Stuart, in Infrared Spectroscopy: Fundamentals and Applications, John Wiley & Sons, Ltd, 2005, DOI: 10.1002/0470011149.ch3, pp. 45-70.

227. P. Eaton and P. West, Atomic Force Microscopy, Oxford University Press, 2010.

228. E. Kopperoinen, M.Sc, Univerisity of Turku, 2006.

229. S.-W. Joo, Surface and Interface Analysis, 2006, **38**, 173-177.

230. F. Shi, S. Tu, F. Fang and T. Li, Arkivoc, 2005, **1**, 137-142.

231. W. E. Feely and E. M. Beavers, Journal of the American Chemical Society, 1959, **81**, 4004-4007.

232. E. Leary, S. J. Higgins, H. v. Zalinge, W. Haiss, R. J. Nichols, S. Nygaard, J. O. Jeppesen and J. Ulstrup, Journal of the American Chemical Society, 2008, **130**, 12204-12205.

233. H. M. Osorio, S. Catarelli, P. Cea, J. B. Gluyas, F. Hartl, S. J. Higgins, E. Leary, P. J. Low, S. Martin, R. J. Nichols, J. Tory, J. Ulstrup, A. Vezzoli, D. C. Milan and Q. Zeng, Journal of the American Chemical Society, 2015, **137**, 14319-14328.

234. J. Kankare and E.-L. Kupila, J. Electroanal. Chem., 1992, **332**, 167-181.